

Vanja Revold Olberg

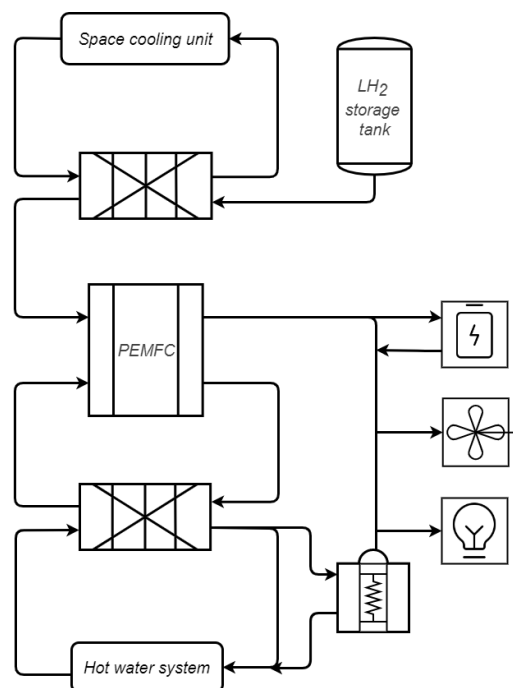
Thermal energy recovery and storage for a hydrogen fuel cell and battery driven cruise ship

Master's thesis in Energy and Environment

Supervisor: Armin Hafner

Co-supervisor: Muhammad Zahid Saeed

June 2022



Created by author

Vanja Revold Olberg

Thermal energy recovery and storage for a hydrogen fuel cell and battery driven cruise ship

Master's thesis in Energy and Environment
Supervisor: Armin Hafner
Co-supervisor: Muhammad Zahid Saeed
June 2022

Norwegian University of Science and Technology
Faculty of Engineering
Department of Energy and Process Engineering

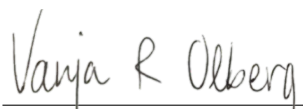
Preface

This master's thesis is the final part of the Energy and Environmental Engineering programme at the Norwegian University of Science and Technology (NTNU) in Trondheim, Norway. The thesis makes up 30 ECTS of the two-year master's programme. The project was supervised by Professor Armin Hafner from the Department of Energy and Process Engineering, with the co-supervision of PhD candidate Muhammad Zahid Saeed from the same department.

The thesis was initiated by the CruiZE project (Cruising towards Zero Emissions), which is a collaboration between SINTEF and NTNU. Its goal is to reduce greenhouse gas emissions in the cruise ship industry. This can be achieved through renewable energy sources and by reducing the overall energy use on board the cruise ship with energy saving strategies. The goal of this thesis is thus to develop and evaluate such solutions for cruise ship applications.

I wish to thank my first supervisor, Armin Hafner, for his advice and support through the year, and my second supervisor, Muhammad Zahid Saeed, for his feedback on my thesis and guidance with the simulation program Modelica. I also wish to thank Cecilia Gabriellii from SINTEF Energy Research for her valuable feedback.

Trondheim, 01 July 2022


Vanja Revold Olberg

Abstract

The maritime sector is facing stricter regulations relating to greenhouse gas emissions, evident from the prospect of zero-emission ports along the Norwegian coast by 2026 and requirements made by the International Maritime Organization (IMO). Two measures that can be made to meet these regulations are propulsion based on renewable energy in place of fossil fuels and reducing the total energy consumption on board, which are significant in cruise ships. This thesis develops a solution encompassing both these initiatives with the research question being the following: *How should a hybrid hydrogen fuel cell and battery system be developed for a cruise ship, and how would thermal energy recovery and storage affect its capacity and performance?*

To answer the research question, a fully electrical energy system was developed for a real-life reference cruise ship named Birka, which operates in Sweden. The system consists of a hybrid high-temperature hydrogen fuel cell (HFC) and battery system which was evaluated in terms of system design, capacity, and performance. The fuel cell is fuelled by liquid hydrogen (LH₂) stored at a cryogenic temperature in tanks on board.

Models of thermal energy recovery (TER) from the system were also developed in Modelica. They represent TER from both the hydrogen fuel cell and from the regasification process of the LH₂ used to supply the HFC. For the heat energy recovery system, the temperature of the fuel cell stack was kept relatively stable around its set-point of 180 °C. This led to heat energy recovery in form of high-temperature domestic hot water of 90 °C, which can be used for the thermal energy hotel demands. The cold thermal energy recovery can be supplied to a CO₂ refrigeration unit to meet space cooling demand. All models can easily be expanded and combined for more complete system solutions.

The implementation of TER resulted in 30.1% less annual fuel consumption, 30.8% less fuel storage capacity needed, and 32.7% less installed capacity necessary for the HFC and battery. When including thermal energy storage (TES) in addition to the TER, the fuel consumption was reduced by 33.8% and the storage capacity by 33.9%. The HFC and battery capacity was unchanged with TES. When including a CO₂ refrigeration heat pump unit, the space cooling demand can be reduced by 80.9% with TER and covered completely when including TES as well. The conclusion drawn from this is that TER would be highly beneficial for a hydrogen fuel cell system, while TES requires further profitability analysis. When including TER and TES, the final installed capacity of the HFC is 7.30 MW, and for the battery it is 1.63 MW, adding up to a total of 8.93 MW.

For future projects, the developed models can be further optimised, expanded, or combined to achieve a deeper analysis of the TER and TES effects. Economic and environmental analyses must also be performed on the proposed system to determine its profitability. However, the results from this thesis show that hydrogen fuel cells with thermal energy recovery can be feasible for maritime applications in future projects with further development and research.

Sammendrag

Den maritime sektoren møter strengere krav i forbindelse med klimagassutslipp basert på fremtidsplaner om nullutslippshavner langs Norges kyst innen 2026 og restriksjoner pålagt av Den internasjonale sjøfartsorganisasjonen (IMO). To tiltak som kan gjøres for å møte disse målene inkluderer skip drevet av fornybar energi i stedet for fossilt brensel og reduksjon av det totale energiforbruket om bord, noe som er signifikant på cruiseskip. Denne oppgaven utvikler en løsning som omfatter begge disse tiltakene med følgende problemstilling: *Hvordan bør et hydrogenbrenselcelle- og batterisystem utvikles for et cruiseskip, og hvordan vil gjenvinning og lagring av termisk energi påvirke kapasiteten og ytelsen til systemet?*

For å svare på problemstillingen ble et elektrisk system utviklet for et reelt referansecruiseskip, Birka, som opererer i Sverige. Systemet består av en hybrid av en høytemperatur hydrogenbrenselcelle og et batterisystem som ble evaluert på bakgrunn av systemdesign, kapasitet og ytelse. Brenselcellen driftes av flytende hydrogen (LH2) som lagres under kryogen temperatur i tanker om bord.

Modeller av termisk energigjenvinning (TER) fra systemet ble også utviklet i Modelica. De representerer TER fra både hydrogenbrenselcellen og fra fordampningsprosessen til LH2 som leveres til HFC-en. I systemet for varmegjenvinning holdt temperaturen til brenselcellen seg relativt stabil rundt settpunktet på 180 °C. Dette ledet til varmegjenvinning i form av høytemperatur varmtvann på 90 °C, som kan brukes til å dekke varmeenergiebehovet om bord. Kuldegjenvinningen kan bli levert til en CO₂-kjøleenhet for å møte behovet for romkjøling. Alle modellene kan enkelt utvides og kombineres for å oppnå mer fullverdige løsninger.

Implementasjonen av TER resulterte i 30,1 % mindre årlig brenselforbruk, 30,8 % mindre behov for lagringskapasitet for brensel og 32,7 % mindre kapasitet nødvendig for HFC-en og batteriet. Ved inkludering av lagring av termisk energi (TES) i tillegg til TER, ble brenselforbruket redusert med 33,8 % og lagringskapasiteten med 33,9 %. Kapasiteten til HFC-en og batteriet var uendret med TES. Ved inkludering av CO₂-kjøleenheten ble romkjølingsbehovet redusert med 80,9 % med TER og helt dekket ved inkludering av TES i tillegg. Konklusjonen som ble dratt av dette er at TER vil være høyst nyttig for et system med hydrogenbrenselcelle, mens TES krever videre lønnsomhetsanalyse. Med TER og TES inkludert ble den resulterende kapasiteten til HFC-en 7,30 MW, og for batteriet er den 1,63 MW, som gir samlet kapasitet på 8,93 MW.

For fremtidige prosjekter kan modellene bli videre optimalisert, utvidet eller kombinert for å oppnå en dypere analyse av effekten til TER og TES. Økonomiske og miljømessige analyser må utføres på det foreslåtte systemet for å kunne bestemme lønnsomheten. Likevel viser resultatene fra denne oppgaven at hydrogenbrenselceller med varmegjenvinning kan være gjennomførbart for maritim sektor i fremtidige prosjekter ved videre utvikling og forskning.

Project Description

This is the project description provided for the pre-project for this thesis, with the project aim of the final thesis added at the end.

Background and Objective:

Cruise ships use a lot of energy and represent an energy-intensive segment of the shipping industry. In Norway, the annual energy use of cruise ships has been estimated to about 5 TWh, corresponding to 8% of the total energy used for transport. The energy demand of cruise ships is traditionally supplied by burning fossil fuels, leading to a higher carbon footprint per passenger in addition to air pollution in major ports worldwide. Due to this, the cruise industry is facing ever more stringent regulations to emissions. Current efforts towards 'greener' and more environmentally friendly cruise ships have a large extent focused on novel hybrid propulsion systems based on liquid natural gas (LNG), batteries and hydrogen. New propulsion systems, however, imply a significant change in the energy system of the ships regarding waste heat characteristics and heating/cooling loads.

For cruise ships, the energy consumption of the hotel facilities on board the ships may constitute up to 40% of the ship's total energy usage. This makes cruise ships significantly different from other shipping segments where the energy consumption is dominated by the propulsion system.

The natural refrigerant CO₂ for cooling and heating is an attractive choice due to its compact units, non-toxic nature, and non-flammability, all being primary concerns on a cruise ship.

In close cooperation between NTNU, SINTEF, and industrial partners, the project aims to develop and evaluate thermal designs for hydrogen fuel cell and battery-driven cruise. The models should include the surplus heat, cold recovery, and their integration with the CO₂ refrigeration system.

The following tasks are to be considered:

1. Review of relevant literature e.g., Refrigeration system (comfort and provision cooling) for cruise ship, thermal management of hydrogen fuel cells and electric batteries, and potential for thermal energy storage.
2. Develop design specifications of the reference case, including CO₂ refrigeration system and their integration with thermal systems.
3. Develop basic skills in Modelica/Dymola modelling environment.
4. Perform initial simulations of the different parts of the energy system.
5. Analyse and discuss the results in terms of system performance, energy consumption and thermal energy storage potential/demand.
6. Project work report including chapters discussion, summary, and proposal for further work

Project Aim:

The project aims to develop and evaluate thermal designs for a hydrogen fuel cell and battery-driven cruise ship. Investigate battery influence and recovered heat application. Develop a load profile with details on the type of loads and which can be covered with heat and cold energy recovery. The models should include the surplus heat, cold recovery, and their integration with the CO₂ refrigeration system. Analyse and discuss the simulation results in terms of system performance, energy consumption, and thermal energy storage potential/demand.

Contents

Preface	i
Abstract	iii
Sammendrag	v
Project Description	vii
Abbreviations	vi
Figures	vii
Tables	viii
1 Introduction	2
1.1 Background	2
1.2 Research Question and Objectives	3
1.3 Scope and Limitations	3
1.4 Project Outline	4
2 Literature Study	5
2.1 Cruise Ship Reference Case	5
2.2 CO ₂ Refrigeration	8
2.3 Hydrogen Fuel Cells	10
2.4 Fuel Cell Thermal Management	11
2.4.1 Heat Production	11
2.4.2 Coolant Options	12
2.4.3 Heat Energy Application Areas	14
2.5 Hydrogen Liquefaction and Regasification	14
2.6 Battery and Fuel Cell Combination	15
2.7 Thermal Energy Storage	16
2.7.1 Peak Shaving and Load Shifting	16
2.7.2 TES Technologies	16
3 Methodology	18
3.1 System Design and Capacity	18
3.1.1 Energy System Design	18
3.1.2 Power Demand	19
3.1.3 Fuel Consumption	20
3.1.4 Thermal Energy Recovery Method	20
3.1.5 Thermal Energy Storage Method	22
3.1.6 Battery Implementation	22
3.2 Dynamic Calculations	23
3.2.1 Heat Energy Recovery Simulation	23
3.2.2 Cold Energy Recovery Simulation	24

3.2.3	Combined Recovery Model	26
4	Results	27
4.1	Reference Case Energy Demand	27
4.2	Thermal Energy Recovery	30
4.2.1	Heat Energy Recovery	30
4.2.2	Cold Energy Recovery	33
4.3	Thermal Energy Storage	34
4.3.1	Heat energy storage	34
4.3.2	Cold Energy Storage	35
4.4	Fuel Demand Evaluation	35
4.5	Battery Influence on System	37
4.6	Dynamic Calculations	38
4.6.1	Coolant Comparison	38
4.6.2	Heat Energy Recovery Model	40
4.6.3	Cold Energy Recovery Model	45
5	Discussion	50
5.1	System Design	50
5.2	Reference Case Evaluation	51
5.3	Thermal Recovery and Storage	52
5.4	System Capacity and Battery Influence	53
5.5	Simulation Evaluation	54
5.5.1	Heat Transfer Fluid Choice	54
5.5.2	Heat Energy Recovery Model Evaluation	55
5.5.3	Cold Energy Recovery Model Evaluation	56
6	Conclusion	58
7	Further Work	59
	Appendices	64
A	Modelica simulation models	64

List of Abbreviations

Abbreviation	Description
BC	Base Case
CHP	Combined Heat and Power
COP	Coefficient Of Performance
DHW	Domestic Hot Water
EG	Ethylene Glycol
GHG	Greenhouse Gases
GWP	Global Warming Potential
HFC	Hydrogen Fuel Cell
HT	High Temperature
HVAC	Heating, Ventilation, and Air-Conditioning
LT	Low Temperature
MFR	Mass Flow Rate
PCM	Phase Change Material
PEM	Proton Exchange Membrane
PG	Propylene Glycol
TER	Thermal Energy Recovery
TES	Thermal Energy Storage

List of Figures

1	Speed profile of reference cruise ship	5
2	Schematic diagram of compression chiller	8
3	PEMFC working principle	10
4	Sankey diagram for a PEMFC	12
5	Liquefaction and regasification process of hydrogen	15
6	Simple diagram of FC stack cooling system	18
7	Modelica model of TER from the HFC stack	24
8	Modelica model of cold energy recovery directly with water.	25
9	Modelica model of cold energy recovery with secondary stream.	26
10	The combined power demand of the cruise ship for all scenarios	27
11	Energy demands of the reference cruise ship	28
12	Power demands at 9 am for all scenarios.	29
13	The heating power demands and daily recoverable heat energy	30
14	Daily energy demand for each scenario and daily recoverable heat energy.	31
15	Power demands at 9 am for all scenarios.	32
16	Total power demand for all summer, spring/fall, and winter scenario when no thermal energy storage is used.	32
17	Cooling demand, cold energy that can be recovered, and the cooling power from a heat pump with $COP = 5$	33
18	Daily available recoverable cold energy and the daily space cooling demand.	34
19	Maximum heating demand for all cases.	35
20	The effect of including TER and TES on annual fuel consumption, fuel storage capacity, and energy system capacity.	37
21	Total power demand with peak shifting from battery implementation.	38
22	Cooling circuit and secondary stream mass flow rates for three coolants.	39
23	Cooling circuit and secondary stream mass flow rates for water and PG/W.	39
24	Modelica heat energy recovery model values at maximum heat production.	41
25	The fuel cell stack's heat production.	41
26	Simulated temperature for the fuel cell stack outlet flow.	42
27	Simulated temperature for the HT recovery stream water outlet.	42
28	Simulated temperature for the LT recovery stream water outlet.	43
29	Simulated mass flow rate for the cooling circuit.	43
30	Simulated mass flow rate for the HT recovery stream.	44
31	Simulated mass flow rate for the LT recovery stream.	44
32	Enthalpy of the outlet stream.	45
33	Plot of the hydrogen fuel mass flow rate during simulation.	46
34	Modelica cold energy recovery model values at maximum hydrogen fuel mass flow rate.	46
35	Simulated temperature for outlet hydrogen stream.	47
36	Simulated temperature for the outlet recovery stream.	47
37	Simulated mass flow rate for the cold energy recovery stream.	48
38	Plot of the cooling demand during simulation.	49
39	Plot of the temperatures in the second cold energy recovery circuit.	49

40	Simple heat energy recovery model.	64
41	Cold energy recovery model with CO ₂	64
42	Cold energy recovery with two recovery streams.	65
43	Combined heat and cold energy recovery.	65

List of Tables

1	Power demand profile for reference cruise ship	6
2	Total installed power of the energy components for the reference case [1].	8
3	Properties of LH ₂	11
4	Properties of Therminol heat transfer fluids	13
5	Peak and average power demands for all scenarios.	29
6	Daily energy demand for each scenario and annual energy demand.	29
7	Daily heat energy demand for all scenarios and cases.	31
8	Daily heat energy demand for all scenarios and cases.	34
9	Daily and annual cooling demand for all cases	35
10	The daily energy demands for each scenario.	36
11	Annual energy demands for the different energy categories for all three cases.	36
12	Daily and annual fuel consumption.	36
13	The reduction of annual fuel consumption, fuel storage capacity, and energy system capacity when including TER and TES.	37
14	The heat flow load profile for the coolant testing.	38
15	The heat flow loads applied to the simulated fuel cell stack.	40
16	The hydrogen fuel mass flow rate profile applied to the cold energy recovery model.	45
17	The cooling demand load profile applied to the cold energy recovery model.	48

1 Introduction

1.1 Background

The maritime sector, including cruise ships, faces stricter regulations on greenhouse gas (GHG) emissions. In 2010, the total CO₂ emitted due to the shipping industry was approximately 1 billion tons, which corresponded to about 3%-5% of global CO₂ emissions [2]. The International Maritime Organisation (IMO) set a target to reduce the CO₂ emissions per shipping transport work by at least 40% by 2030 and 70% by 2050, compared to 2008 [3]. Not only CO₂ emissions should be regulated, but also other environmentally harmful gasses like NO_x and SO₂, which pose a significant issue in ships running on fuel oil. Regulations from the European Union (EU) aim to reduce SO₂ emissions in sensitive sea areas, including the Norwegian coast [2], and the IMO targets zero emissions in Norwegian tourist fjords from 2026 [4]. Port of Oslo aims to be emission free in the long run [5], and the Norwegian Maritime Authority (NMA) requires zero emissions in the World Heritage fjords, of which Norwegian fjords qualify, by the year 2026 [6]. Emission reductions in the maritime sector is thus extremely relevant. One of the efforts to meet these restrictions is the project CruIZE (Cruising towards Zero Emissions), a collaboration between SINTEF and the Norwegian University of Science and Technology (NTNU), in addition to Carnival Corporation & plc and other Norwegian cruise shipping suppliers [7]. Apart from minimising emissions, the main focus of the project is to reduce the total energy use of a typical ship by 10-20% [7].

A large contributor to cruise ship emissions is propulsion based on fossil fuels, so an obvious step towards meeting regulations is switching to a renewable energy source. The switch to liquid natural gas (LNG) has reduced NO_x and SO₂ emissions, and although CO₂ emissions are also reduced compared to fossil fuels, there are still emissions. A better solution is therefore electric propulsion, assuming the electricity has been produced with renewable methods. The most common energy storage methods in transportation for electricity supply are batteries and hydrogen. Hydrogen fuel cells (HFC) pose issues such as complicated storage for the hydrogen, high investment costs, relatively short lifetime, slow transient behaviour, and a lack of fuel infrastructure [8]. However, the benefits of a HFC, which apart from zero emissions during operation, include silent operation, good part load performance, and high fuel efficiency, suggests that further research and development of the technology is not only worth it in the long run, but also necessary [8].

There are also other ways of reducing the cruise ship emissions, e.g., by minimising the total energy demand. The cruise ship passengers require certain energy demands for comfort, like heating, ventilation, and air conditioning (HVAC), as well as electrical equipment and domestic hot water (DHW). These hotel loads make up approximately 40% of the ship's total energy demand, meaning significant results might be achieved through more efficient energy usage [9]. One solution is recovery of thermal energy from the different operations which otherwise goes to waste, with the addition of thermal energy storage (TES) for further energy demand control. These are the solutions that will be researched in this project.

1.2 Research Question and Objectives

The goal of this project is to contribute to the reduction of energy use and GHG emissions in the cruise ship sector. This will be achieved by evaluating solutions which can reduce energy demand in cruise ships based on renewable energy production and energy recovery designed specifically for cruise ships. The primary focus of this project is the research and evaluation of a hydrogen fuel cell (HFC) based system for energy production for a cruise ship. The HFC will be supplemented with a battery as this brings several benefits in terms of operational reliability and profitability. Thermal energy recovery from the proposed system will be evaluated as well, in addition to thermal storage to optimise the energy system performance. Based on this, this thesis will answer the following research question:

How should a hybrid hydrogen fuel cell and battery system be developed for a cruise ship, and how would thermal energy recovery and storage affect its capacity and performance?

Several objectives are listed below to help provide a thorough answer to the research question. They will be achieved through literature study, evaluation, calculations, and simulations. Firstly, different technologies for HFCs and batteries will be reviewed for cruise ship applications. The capacity of such a system will be evaluated and the thermal management and recovery is simulated.

1. Develop a simple design for the hybrid HFC and battery system.
2. Determine the most appropriate HFC technology for the system.
3. Determine the capacities needed for the HFC and battery.
4. Evaluate the thermal management of the HFC system.
5. Evaluate the thermal energy recovery from the HFC system and its effect on the capacity and fuel consumption.
6. Evaluate the potential for thermal energy storage and how it will affect the system's capacity and fuel consumption.
7. Consider the integration of the hybrid propulsion system with a CO₂ refrigeration system.

1.3 Scope and Limitations

The scope of this project includes the objectives above, and the report will be centred around achieving these. Since the technology proposed is relatively unexplored for the marine transportation sector, the work in this project is limited to initial evaluation and calculations regarding the system. Due to the time and resource restrictions, the work is focused on exploration of an energy solution where the system design and operation is the priority. Any thorough analysis of GHG emission and economical aspects connected to the proposed solution is especially important for further consideration but are excluded from the project due to its time restriction. A simulation of the entire system with optimisation

is also highly relevant, but due to the manifold of factors affecting the system, these should be well explored and evaluated first. As all simulation models were developed from scratch, they were kept relatively simple.

1.4 Project Outline

The purpose of the remainder of this thesis is to meet the objectives and answer the research question. First, a literature study covering the most relevant theory needed is presented in Section 2. This section presents the reference case with data for energy demands from a real cruise ship, CO₂ refrigeration for cooling purposes, hydrogen fuel cells with their operation and thermal management, hydrogen liquefaction and regasification processes, batteries in combination with fuel cells, and thermal storage technologies. Following the literature study, the methodology used for the thesis is then presented in Section 3, which includes the system design, calculations, and dynamic simulations. The following results can be found in Section 4. These results are discussed in Section 5, where the objectives and research question are brought up again. Finally, conclusions based on the discussion are drawn in Section 6, followed by suggestions for future work in Section 7.

2 Literature Study

This chapter presents theory found in the literature study relevant to answering the research question and reach the objectives of this project.

2.1 Cruise Ship Reference Case

Power demand data used for calculations in this thesis are collected from a real-life cruise ship called Birka. A reference case is created based on the available data from the literature on different energy demands on the ship. Birka is considered a medium sized cruise ship with the capacity to carry 1800 passengers, and it offers facilities like restaurants, pools, and clubs. The cruise ship travels between Stockholm and Mariehamn in Sweden. The speed of the ship during its 24-hour round-trip is plotted in Figure 1. Birka is docked in Stockholm from 4 PM to 6 PM, and after leaving port it sails for six hours before stopping at the open sea for a few hours. It then enters Mariehamn at 8 in the morning and stays for one hour. At 9 AM it returns to Stockholm [10].

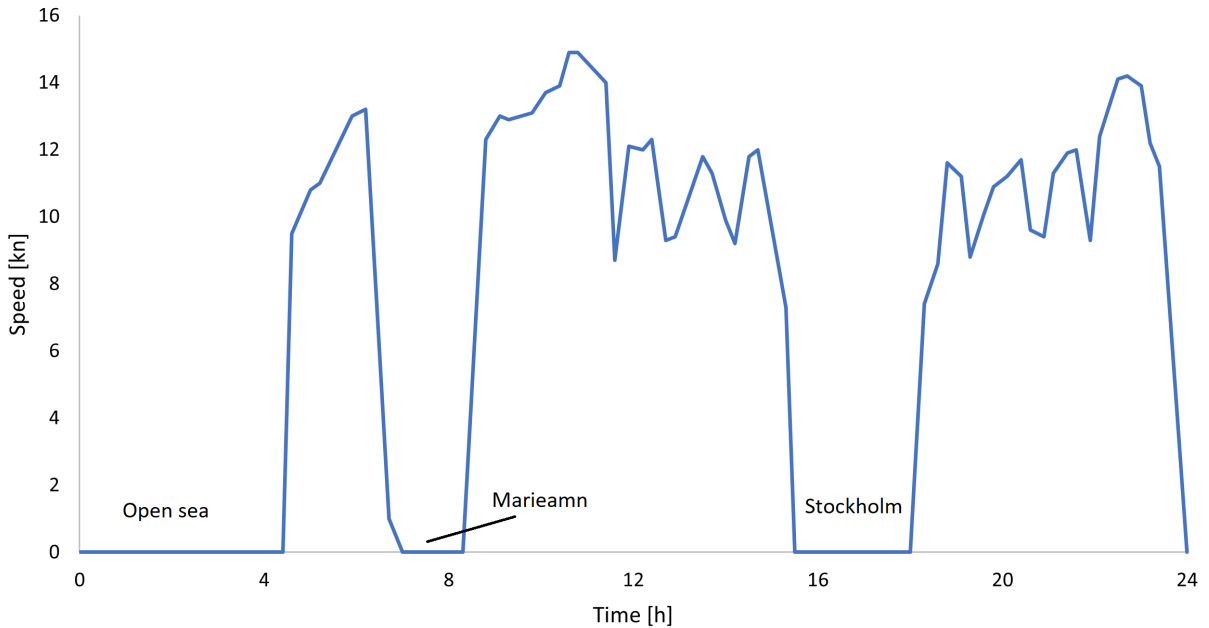


Figure 1: Speed profile of reference cruise ship. Based on [1].

The energy demand of a cruise ship can be categorised into three different purposes, which are 1) propulsion, 2) auxiliary, and 3) hotel. The propulsion demand will be either mechanical or electrical, depending on the propulsion equipment of the ship, and varies depending on the speed and manoeuvring of the ship. The auxiliary electrical demand is typically much lower and constant whether the ship is sailing or not. The hotel energy loads cover the passengers' needs and for a cruise ship, and they typically make up approximately 40% of the ship's total energy demand [9]. The hotel loads fundamentally consist of domestic hot water (DHW) heating, space heating, air conditioning with cooling, provision cooling and freezing, and energy for various electrical equipment like lighting and fans.

The amount of energy needed for each of the categories varies depending on the cruise ship’s capacity, facilities, propulsion system, etc. For this project, most calculations and evaluations regarding the energy demand will be based on data from the Birka cruise ship described above. The energy demand data provided from the ship are distributed between mechanical load (for propulsion), auxiliary electricity load (for all electrical equipment), heating load (for space heating and domestic hot water), and cooling load (for space cooling).

The specific data on the energy demands for Birka are presented in Table 1. The table data is gathered from Table 3 in the paper published by Baldi et al. [1] and from Figure 4 in the paper by Ancona et al. [10]. The table provides data for all allocated power demands of the cruise ship, including propulsion (P_{mech}), auxiliary electricity (P_{aux}), space cooling (P_{cool}), and heating demands for spring/fall ($P_{heat(s/f)}$), summer ($P_{heat(s)}$), and winter conditions ($P_{heat(w)}$). When comparing Table 1 with the speed profile illustrated in Figure 1, it can be assumed that the mechanical energy demand is zero when the ship is docked, while reaching its maximum at 9 am when departing from Mariehamn. The cooling demand is relatively constant around 1000 kW regardless of the ship’s movements, and the same applies to the auxiliary electricity demand which is also relatively stable. The heating demand change more drastically as it depends on the passengers’ needs, which change throughout the day.

Table 1: Power demands of the cruise ship during different hours of the day, all given in kW.

Hour	P_{mech}	P_{aux}	$P_{heat(s/f)}$	$P_{heat(s)}$	$P_{heat(w)}$	$P_{cool(s)}$
1	0	1502	1091	736	2093	1047
2	0	1485	1129	720	2162	883
3	0	1476	1129	720	2189	933
4	0	1540	2634	736	5012	883
5	2075	1551	3763	1701	7229	851
6	2363	1790	3726	2389	7146	982
7	0	1713	3650	2356	6981	1194
8	4305	1824	2107	2339	4062	1374
9	6343	1817	2070	1391	3966	1227
10	6218	1844	1957	1342	3745	1112
11	3800	1835	1882	1243	3621	1145
12	3012	1834	2220	1211	4227	1129
13	3320	1834	2145	1423	4131	1227
14	2940	1815	2145	1374	4103	1014
15	0	1880	2145	1374	4103	916
16	0	1849	2597	1374	4957	998
17	0	1945	2672	1669	5122	982
18	2601	1830	3312	1701	6361	1047
19	2961	1828	3425	2094	6568	1194
20	3125	1717	3500	2160	6706	1211
21	4023	1638	2597	2241	5053	1112
22	4598	1593	1806	1669	3401	1031
23	3303	1549	1473	1162	2878	982
24	0	1563	1091	982	2093	1096

As the cruise ship operates during all seasons of the year, the heating and cooling loads will vary depending on the environmental conditions. As can be expected for climate in the northern hemisphere, the space heating demand is highest during winter and lowest during summer conditions due to the ambient temperature conditions. Heating demand is present during all seasons, not only winter, due to domestic hot water demand which occur regardless of outdoors conditions. For the Birka case, space cooling demand is assumed to only be needed for summer conditions as it is negligible during the other seasons. The mechanical and auxiliary energy demands are assumed constant for all seasons.

The heating demand is based on hot water demand, which is applied to both the space heating system and domestic hot water consumption by the cruise ship passengers in the cabins. It may also apply to other hot water demanding facilities on board, like for the galley and laundry. Since this data is based on the fact that Birka runs on heavy fuel oil, it is also assumed that some of the heat demand used for heating the fuel oil. Based on the case information, it is assumed that auxiliary boilers with a thermal efficiency of 80% are used for all water heating purposes apart from hot water recovery [10]. There are two auxiliary boilers installed in the reference case cruise ship with a maximum thermal power output of 4500 kW each. Heat energy recovery from the engines is also used to cover the heating demand.

The cooling demand is only applied to space cooling purposes. Provision cooling and freezing is covered by the auxiliary energy demand, which is why the cooling demand presented is only applicable to summer conditions when the ambient temperature exceeds the passengers' comfort range. The cooling power is produced by a compression chiller system and is assumed to have an energy efficiency ratio (EER) of 3.5 under design conditions [10]. The corresponding coefficient of power (COP) can be calculated with Equation 1 [11, 12]. Based on this, the corresponding COP for the system is approximately 1.03. The maximum cooling power output for the chiller is 2000 kW.

$$COP = \frac{EER}{3.41} \quad (1)$$

For cruise ships, there are typically three different types of energy demands, including mechanical, electrical, and thermal. These demands historically have been met with separate systems, with the main engines supplying the propeller, auxiliary engines for electricity production, and boilers for thermal power production [10]. In the reference cruise ship, there are four main engines used for propulsion and four auxiliary engines used for electricity production, all eight fuelled by diesel. The four main engines each have a design power of 5850 kW, while the auxiliary engines are rated at 2760 kW [1].

Table 2: Total installed power of the energy components for the reference case

Installation	Total installed power [kW]
Propulsion	23 400
Auxiliary electricity	11 040
Heating	9000
Cooling	2000

For newer cruise ships it is common to have one system for energy provision which makes it more flexible as engines can be turned on or off depending on the demand. This aids in streamlining the energy provision and reduce the installed capacity. This can also be achieved when using an electrical engine where the engines can be combined and operated more efficiently. This requires a more complicated control strategy.

2.2 CO₂ Refrigeration

Space cooling through air conditioning is necessary on cruise ships which operate during conditions where the temperature becomes uncomfortable for its passengers. As explained in Section 2.1, the ship in the reference case requires space cooling during summer conditions. This can be achieved using a heat pump which removes heat, akin to the system cooling a refrigerator.

Figure 2 illustrates the working principle of a refrigeration heat pump, or compression chiller. It generally consists of a condenser, an evaporator, a compressor, and an expansion valve. The condenser and evaporators are heat exchangers which reject or absorb thermal energy depending on its function. A more detailed description can be found below the figure, based on the numbers in the illustration.

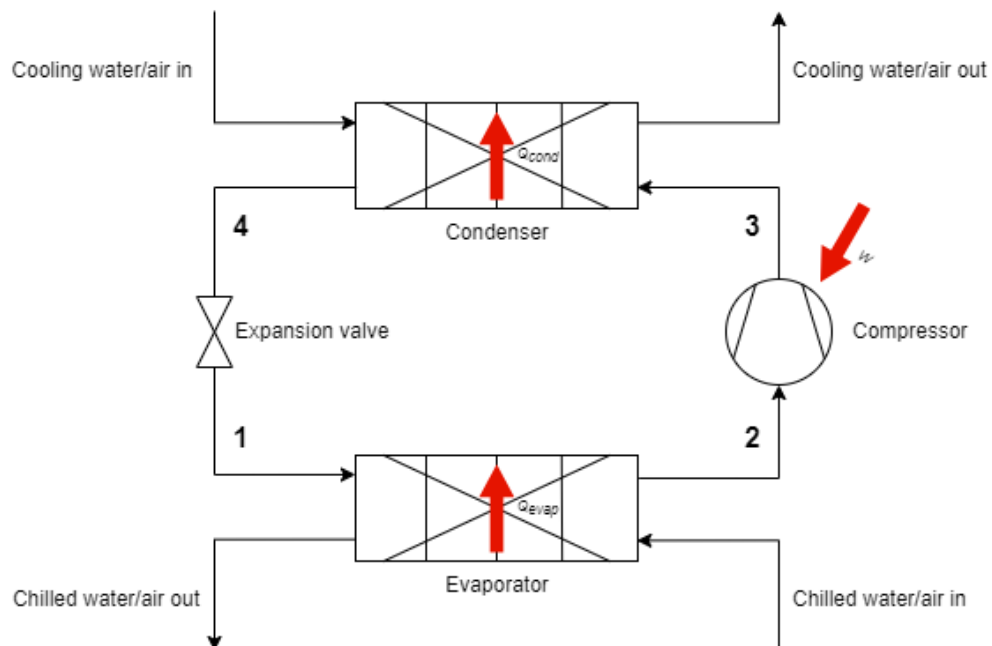


Figure 2: Schematic diagram of compression chiller. Created with diagrams.net, based on [13].

(1-2) Evaporation of medium through heat absorption:

Thermal energy is absorbed due to the heat pump medium having a lower temperature than the chilled air or water entering. The medium evaporates when supplied with the heat flow Q_{evap} .

(2-3) Compression of evaporated medium:

The evaporated working medium is compressed through a compressor driven by electricity, further increasing the working medium temperature.

(3-4) Condensing of medium through heat rejection:

Due to the increased temperature of the working medium, heat is rejected by the condenser to the external environment which has a lower temperature, represented as the heat flow Q_{cond} . As the medium is cooled, it condenses.

(4-1) Expansion of evaporated medium:

The pressure of the condensed medium is reduced through the expansion valve, thus decreasing its temperature further.

The efficiency of such a refrigeration heat pump is indicated by its Coefficient of Power (COP). For the reference ship, the space cooling is provided through a compression chilling system with an EER of 3.5, or a COP of 1.03. The COP is a factor of how much cooling power is provided by the chiller per electrical power input to the compressor in the chiller. A COP of approximately 1 means that when supplying 1 kW to the system, 1 kW of cooling power is provided. The COP value for a chiller is given for specific design conditions and thus depends on the ambient and required temperatures. Air-cooled chillers should have a COP ranging from 2.40 to 3.06 and should be even higher for water-cooled chillers [14].

As shown in Equation 2, the COP is calculated based on the heat removed from the room, Q_{evap} , and the work required by the compressor, W . The maximum theoretical COP can also be calculated in terms of the lower temperature in the room, T_C and the higher temperature outside T_H . This means that the COP can be improved by decreasing the outside temperature, assuming the room temperature is kept constant.

$$COP_{cooling} = \frac{Q_{evap}}{W} = \frac{T_C}{T_H - T_C} \quad (2)$$

When it comes to the working medium used in the compression chiller, different ones can be chosen based on costs, safety, efficiency, and environmental friendliness. A relatively newly developed refrigeration system is one based on CO₂ as its working medium. CO₂ is a natural refrigerant with several advantages over other refrigerants like ammonia and HFCs, including non-toxicity, non-flammability, high compactness, high accessibility, and global warming potential (GWP) of 1 and ozone depletion potential of 0 [9]. For a cruise ship application, the safety aspects are very important due to more complicated evacuation processes in case of accidents, making CO₂ especially attractive. Since CO₂ can be extracted from the atmosphere or directly from production where it is a by-product, it has practically no negative environmental impact.

2.3 Hydrogen Fuel Cells

The reference cruise ship runs on heavy fuel oil. By switching to LNG as a fuel, emissions of both CO_2 and NO_x can be significantly reduced. However, emissions can be further reduced with a renewable energy source like a hydrogen fuel cell (HFC). The HFC produces DC electricity using hydrogen gas as its energy source. Its popularity is increasing because only water and no harmful GHG are produced as side products during operation. If the hydrogen used for fuel is produced with renewable energy sources, the fuel cell is very environmentally friendly, with the only non-carbon neutral factor being the production of the fuel cell itself with all its components. However, compared to fossil fuelled systems, the HFC is an important contributor to reducing GHG emissions.

The most common HFC type is the proton exchange membrane – also called polymer electrolyte membrane – (PEM), due to its advantages like short response time, high power density, and relative low cost and long lifetime. Its electrical efficiency varies in the approximate range of 45-60%, and depends on the operating conditions like temperature, so 50% efficiency is a safe assumption to make [15, 16]. According to Xing et al. [17], the PEM fuel cell is the most applicable to the maritime sector, alongside molten carbonate (MC) and solid oxide (SO) fuel cells. PEMFCs can be classified as low temperature (LT) or high temperature (HT), where HT-PEMFCs typically have a higher efficiency. Optimal temperature for the LT-PEMFC is from 60-80 °C, while the HT-PEMFC is most efficient in the ranges 160-180 °C and can perform up to 200 °C [18, 19]. Thermal energy recovery from HT, compared to LT, is easier because the temperature difference is higher [18]. A PEMFC working principle sketch is shown in Figure 3.

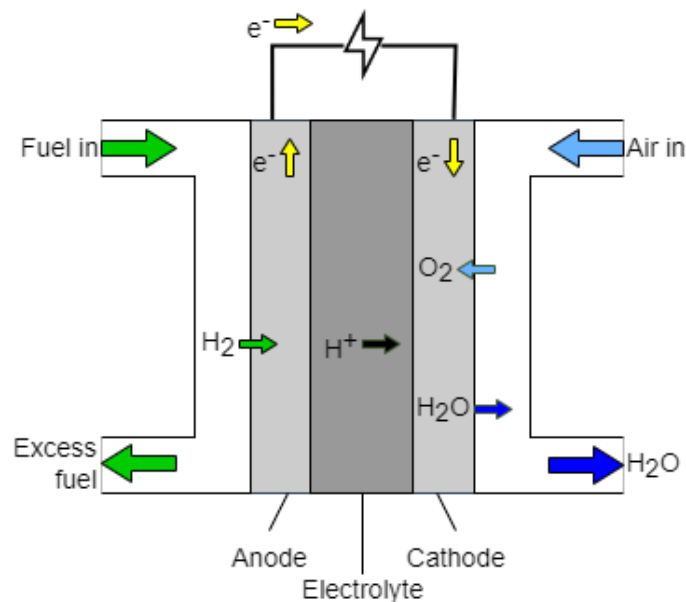


Figure 3: PEMFC working principle. Created with diagrams.net, based on [20].

Simply explained, the PEMFC consists of two electrodes, one cathode and one anode, and an electrolyte which works as a membrane. Hydrogen is fed into the FC at the anode where the single electron in the hydrogen atom is separated from the proton by a catalyst.

Only protons can pass through the membrane, while the electrons are led to the cathode through an external circuit. This current is used to perform work. Finally, the electrons and protons reunite by the cathode in addition to reacting with oxygen being fed into this side of the membrane, forming water. [16, 21]

When it comes to installed power capacity for fuel cells, it is steadily increasing as new solutions are tested and improved. Higher efficiencies, lighter and smaller components, and better storage solutions are all important factors. A hydrogen fuel cell of 3.2 MW is being developed for a shipping vessel in Norway and is planned to be ready in 2023 [22]. This shows that it is not only possible, but highly relevant, with larger hydrogen fuel cell systems for industrial applications in the near future.

There are several methods for storing the hydrogen used to fuel the PEMFC. Hydrogen gas has a high gravimetric energy density compared to other fuels, but a low volumetric energy content due to its low density [23]. For practical purposes, the volume must therefore be reduced. This can be achieved by storing the hydrogen in pressurised tanks or by liquefying it under atmospheric pressure. The pressure in the tanks can be between 100 and 800 bar. The most common storage method is pressurised tanks of 2-300 bar, but for larger scale storage, liquid storage is more suitable as the volumetric density is approximately twice that of hydrogen gas, even at 800 bar. The liquefaction of hydrogen requires cryogenic temperatures as the boiling point of hydrogen gas is $-253\text{ }^{\circ}\text{C}$ at atmospheric pressure [24]. Some properties of liquid hydrogen (LH_2) are presented in Table 3.

Table 3: Some properties of LH_2 .

Property	Value	Source
LHV [MJ kg^{-1}]	120.0	[25]
HHV [MJ kg^{-1}]	141.7	[25]
Gravimetric density [kg L^{-1}]	0.071	[26]
Volumetric density [kg m^{-3}]	70.8	[24]

2.4 Fuel Cell Thermal Management

2.4.1 Heat Production

The hydrogen fuel cell produces heat during operation due to the various losses, which consist of hydrogen crossover, ohmic resistance, mass transportation and activation losses [15]. The efficiency of the HFC is based on the useful energy provided by it divided by the energy stored in the hydrogen used to fuel it, which is calculated based on the higher heating value (HHV) of the liquid hydrogen. According to Nguyen and Shabani [15], the Sankey diagram in Figure 4 shows the typical energy flow in a PEMFC. The percentages are based on the HHV of the hydrogen supplied, and based on this energy one can assume a electric power output of 50%, with 5% of the energy lost due to unreacted hydrogen, 5% is spent on internal water evaporation, 2% to extra reactants, and 2% of the heat is removed by natural convection. This leaves approximately 36% of the energy being released as heat in the fuel cell stack which can be recovered by the cooling system [15].

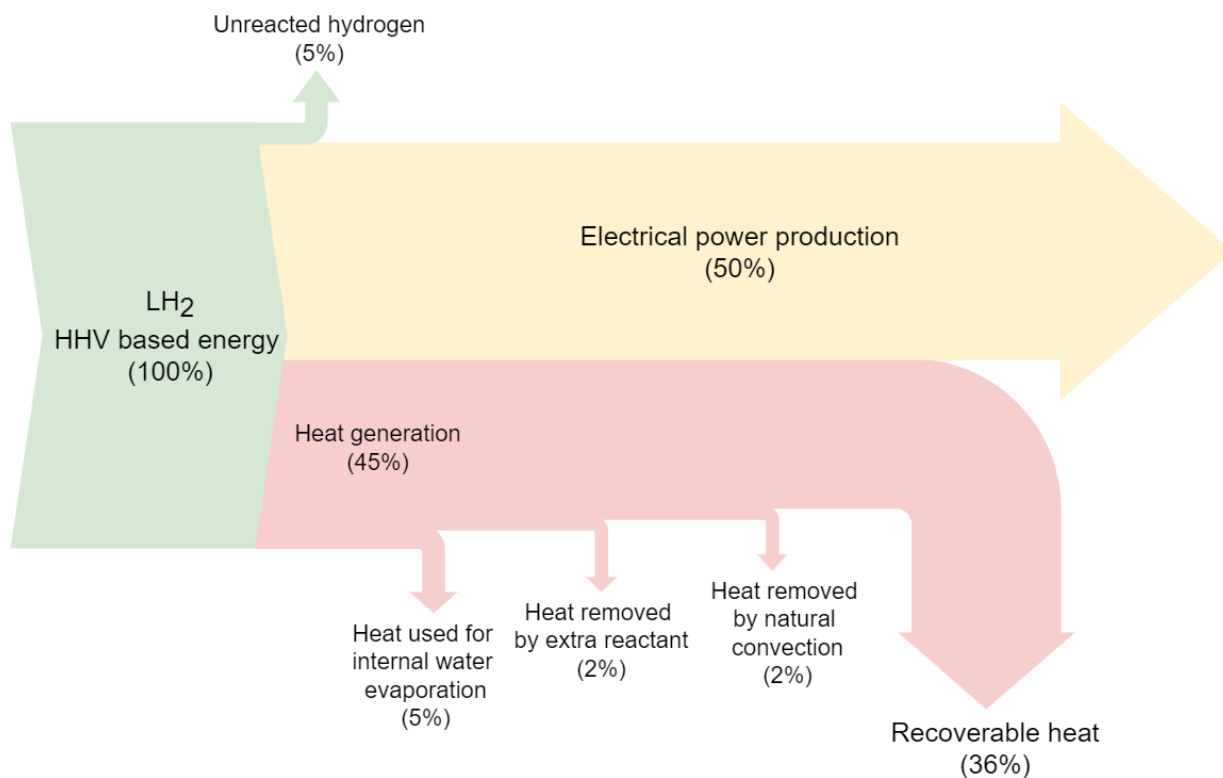


Figure 4: Energy flow diagram for a PEMFC. Created with diagrams.net, based on [15].

The HFC stack heat production must be removed by a cooling system for it to retain a uniform and stable temperature profile. Without this thermal management, the membrane in the cell may overheat and dry out, which reduces the proton conductivity and thereby also the efficiency [18]. The lifetimes of the fuel cell components are also reduced through overheating [27]. The cooling system should regulate the temperature so that it is optimal for the specific fuel cell in use to achieve the best performance. The optimal operational temperature depends on the components used in the fuel cell as well as operational conditions.

There exist various types of thermal management systems for PEMFCs, including sprinklers and circulating air, liquid, and phase change cooling [18]. For a fuel cell with high design power (over 10 kW) or high operating temperature, liquid cooling is very effective due to its higher thermal capacity and thermal conductivity compared to air [15, 27]. Liquid cooling is performed by circulating the coolant through dedicated cooling plates or channels through the FC stack [28], which ensures a more uniform temperature across the entire stack, in addition to removing heat. The heat from the returning coolant is typically rejected by heat exchange through a radiator. Other interesting cooling options for HT-PEM fuel cells are thermo-oil, steam, and pressurised water, but these are less common [29].

2.4.2 Coolant Options

The working fluid used for liquid cooling must meet certain criteria for optimal performance. It should not freeze during operation, and its boiling point should be higher than

the operating temperature of the fuel cell to avoid evaporating [30]. Typically for transportation, the flash point must be greater than 99.33 °C which means that they will be non-flammable for transportation safety purposes [29]. However, the flash point must exceed 60 °C as regulated by NMA [31]. The coolant should also have high thermal conductivity for more efficient heat transfer. In addition, it should not be toxic in case of leakage, and it should have very low environmental impact, including low GHG emissions and GWP.

For a medium temperature range, water is a good coolant choice due to its low cost and high thermal conductivity. However, it has a relatively narrow operating temperature range and will freeze in sub-zero temperature areas and boil at working temperatures above 100 °C. Antifreeze fluids solve the issue with sub-zero temperatures, where a very common working fluid is ethylene glycol (EG), which is mixed with water in different ratios depending on the application [29]. The mixture achieves a much lower freezing point than water alone, and also slightly increases the boiling point, widening the operating temperature range on both sides [15, 29]. Ethylene glycol is, however, toxic to humans, which is why the non-toxic option of propylene glycol (PG) mixed with water is also popular. This mixture gives a slightly narrower operating range, but the difference is relatively small. The downside to these antifreeze coolants is the significant reduction in thermal conductivity, which negatively impacts the efficiency. Since the performance of the coolant depends on the thermal conductivity, much research has been conducted on methods for increasing the conductivity while still keeping a low freezing temperature. This has been achieved by using the antifreeze coolant as a base while adding nano-fluids to it. However, the antifreeze fluids cannot be used for operating temperatures above 107 °C, which would be an issue for a HT-PEMFC.

There are manufacturers who offer heat transfer fluids that can withstand much higher temperatures, well past 300 °C, one of them being Therminol®[32]. The fluid Therminol 66 is the most popular high-temperature, liquid-phase heat transfer fluid and shows high stability. Another is Therminol 59 which is inexpensive and wider temperature operation range. A third is Therminol D-12 which is well suited for lower temperature ranges. The most relevant properties of these three heat transfer fluids are presented in Table 4.

Table 4: Properties of three Therminol heat transfer fluids [33].

Property	Therminol 59	Therminol 66	Therminol D-12
Min. use temperature [°C]	-49	-3	-94
Recommended bulk use temperature [°C]	315	345	230
Normal boiling point [°C]	289	359	192
Flash point [°C]	146	184	62
Thermal conductivity (100 °C) [W m ⁻¹ K ⁻¹]	0.115	0.114	0.097
Thermal conductivity (200 °C) [W m ⁻¹ K ⁻¹]	0.104	0.106	0.077
Specific heat capacity (200 °C) [kJ kg ⁻¹ K ⁻¹]	2.27	2.19	2.84

2.4.3 Heat Energy Application Areas

The heat removed from the HFC stack by the coolant can be recovered, creating a combined heat and power (CHP) system which would increase the overall energy efficiency of the fuel cell system. According to Nguyen and Shabani [15], many studies show that the energy efficiency of a fuel cell system can be increased to 80-90% when combined with heat energy recover. This is called thermal energy recovery (TER).

The recovered heat can be used internally in the FC system, i.e., to preheat the reactants, or removed from the system for domestic hot water heating or storage. There are also other options, like electricity production with the use of thermoelectric generators (TEG), organic Rankine cycles (ORC), or absorption cooling technology [15, 34]. The cooling technique is relevant if cold recovery cannot cover the cooling loads of the cruise ship. However, for a cruise ship application, the simplest and most useful option is probably to use the recovered heat to cover (parts) of the hotel heating loads. Another option applicable to cruise ships is seawater desalination. The distillation should happen at a temperate of 50-90 °C [35], which might be fitting for HFC heat energy recover.

2.5 Hydrogen Liquefaction and Regasification

In addition to TER from the fuel cell stack, also cold can be recovered from the fuelling system [36]. For this case, it is assumed that hydrogen is stored as a liquid, which is achieved by cooling it to at least -253 °C at atmospheric pressure. The liquefaction process is energy intensive due to the cryogenic temperature needed. To increase the overall energy efficiency of the system, part of the energy consumed during the liquefaction process can be recovered during operation. This principle has already been applied to liquid natural gas (LNG) used as a fuel on many modern cruise ships [37, 38], which is also stored at a cryogenic temperature (below -162 °C), and since LH₂ is stored at an even lower temperature, the potential is there for a similar solution.

Before entering the fuel cell, the hydrogen must be evaporated from its liquid state and reach an ambient temperature. Traditionally, this regasification has been performed using heat exchange with ambient air, where the cold outlet air stream is released to the environment [39]. However, there is potential for energy saving by utilising the removed cold on board the cruise ship. The whole process simplified is illustrated in Figure 5.

The most relevant purposes for cold recovery include HVAC applications, like space cooling through the air conditioner, freezing and cooling of products, power production with an ORC unit, and cooling of the fuel cell and battery [40]. For cruise ships operating in warm climates, the air conditioning cooling load can be significant. Cold recovery from the fuel cell system should therefore reduce the overall energy demand of the ship [9].

The enthalpy changes resulting from regasification of LNG and LH₂ are approximately 1.7% and 3.2% of their lower heating values, respectively [39]. The LHV of LNG is 48.6 MJ per kg and for LH₂ it is 120 MJ per kg. According to other sources, the cold energy that can be recovered during regasification of LNG is around 830-860 kJ per kg [37, 41].

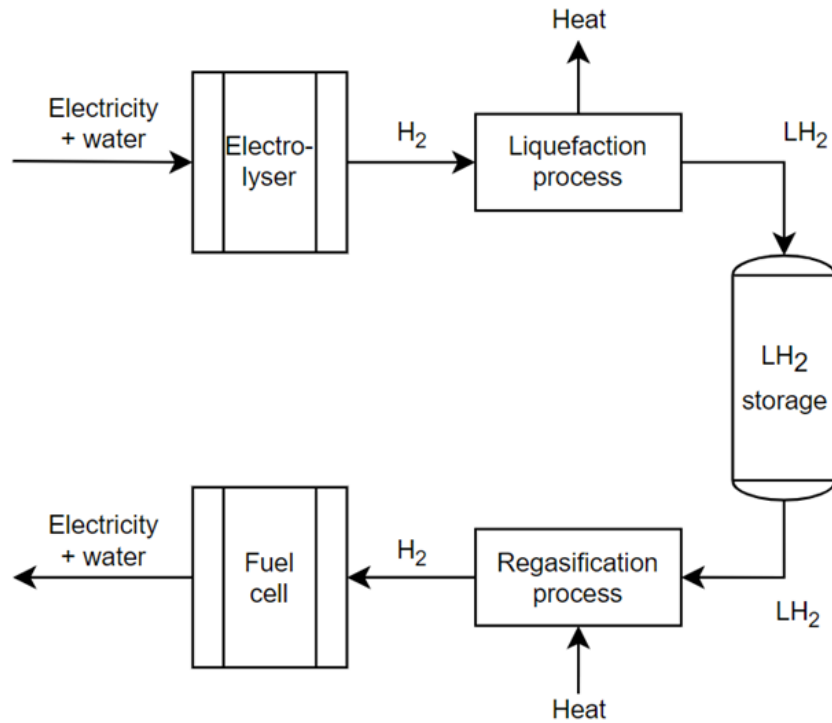


Figure 5: Liquefaction and regasification process of hydrogen. Created with diagrams.net.

2.6 Battery and Fuel Cell Combination

It is necessary to combine the HFC system with a battery system to achieve optimal operation [27]. This is due to several reasons like peak load coverage and better performance of the fuel cell, which will be further explained in this section.

Firstly, a battery should cover the power demand peaks of the ship while the HFC system covers the base with peak shaving, which is further presented in Section 2.7. This is because the relative costs for the HFC system is higher, so over-dimensioning this system to cover the highest peak loads while a large capacity is not used for the majority of the operation is very expensive. Therefore, the PEMFC should cover the base load, which is average propulsion load and some base hotel loads, while the battery covers the top loads.

Secondly, a fuel cell shows poor dynamic response to changing power demands, because abrupt changes in the power demand causes stress on the membrane, reducing the performance [2]. When the power demand suddenly increases, the battery system can cover the initial increase, letting the FC increase the capacity at a slower rate. On the other hand, when the power demand decreases abruptly, the FC does not have to reduce its capacity immediately, but instead adapt slower. The additional electricity produced can be used to charge the battery, meaning that the FC is given more time to adapt without any energy being wasted. Such a combination is therefore highly beneficial and will typically be worth the additional initial investment costs for the battery pack.

2.7 Thermal Energy Storage

Thermal energy storage (TES) technology is used for storing excess energy produced during times of relatively low demand for periods when the thermal energy demand is higher [42]. TES involves charging a medium with thermal energy from a source, which is then stored inside the medium until it is needed, at which point the energy is discharged into a thermal sink [43]. The purpose of TES is to reduce the needed installed capacity of an energy system and to minimise energy wastage. This happens through peak shaving.

2.7.1 Peak Shaving and Load Shifting

TES can be used for peak shaving of the thermal power demand load curve experience by the energy production system. This happens when the stored energy is used to cover part of the thermal demand during times of peak power demand to alleviate the production needed from the system [44]. Load shifting consists of redistributing the amount of available energy to better fit the energy demand [45]. This is achieved by overproduction during periods of low demand, storing the excess energy, and utilising it during periods of high demand.

If one assumes for a fully electrical cruise ship that the thermal demand is met (partly) by electrical boilers provided power directly by the fuel cell system, TES can be used for peak shaving. During periods where the fuel cell must deliver the highest power level, where part of this power is needed by the electric boilers, the thermal demand can be met instead with stored thermal energy. This would reduce the overall power needed from the fuel cell. Since the fuel cell is dimensioned based on the maximum power needed, its installed capacity may be reduced accordingly, thus saving investment costs, space and weight.

In practice, this means that during peak power demand periods of the day, stored energy can be used in addition to the energy supply system (e.g., a fuel cell and battery combination), thus reducing the system's necessary capacity and saving investment costs. Outside of peak demand hours, the HFC will have available capacity which can be used to produce additional energy to be stored for later. The fuel cell efficiency is typically the highest when the FC operates close to its rated power, meaning that the FC should charge the battery or TES whenever the full rated power is not needed to fill the cruise ship's energy demand [15]. This load shifting can be highly beneficial to the systems performance and cost.

2.7.2 TES Technologies

Thermal energy can be stored as sensible or latent heat/cold energy. Sensible energy storage happens when the TES material changes temperature proportionally to the energy supplied/removed, without any phase change within the material. Latent energy storage, on the other hand, involves a phase changing material, meaning that the temperature is constant during (dis)charging. A third TES storage method is thermochemical heat, but this is not yet commercialised. TES can be used for storing both "hot" and "cold" energy, depending on the application and technology.

For sensible TES, water is a common storage medium as it is inexpensive with a relatively good heat capacity. It is also useful when covering domestic hot water demands as it can be used directly without transferring the thermal energy to another medium. It is common to store the hot water in tanks with the use of natural stratification. This happens when the higher temperature water floats to the top due to its lower density. The mixing zone separating the hot and cold water is called a thermocline and should be narrow to increase the storage efficiency [46]. This is achieved by using diffusers in the hot and cold zone which controls the speed of the inlet water, reducing mixing of the two layers. Assuming the tank is used for hot water storage, charging is performed by adding hot water through a nozzle at top of the tank while cold water is removed through a nozzle at the bottom. Discharging is performed by the opposite process where hot water is removed. Assuming a small mixing zone, stratified tanks are well suited for large storage capacity above ground [43], but would probably be a challenge for cruise ship applications due to the ships movement which would disturb the thermocline. Other options for TES must therefore be considered.

When it comes to storing cold energy, this can be done through ice formation. Typically, there is a tube system where the goal is to have a low volume compared to surface ratio to ensure more uniform freezing. The storage is discharged by letting the ice melt by running a warmer working medium through the tubing system. A PCM can also be considered for cold thermal energy storage [47], although water is a good option due to low cost.

3 Methodology

The methodology described in this section is the one applied to reach the objectives, and thus also answer the research question. It covers a proposed system design, calculations, and simulations of different energy recovery systems.

3.1 System Design and Capacity

3.1.1 Energy System Design

A simplified illustration of the total energy production and TER systems is illustrated in Figure 6. Green lines represent hydrogen, yellow is electric current, red is hot stream, while blue is cold stream. The figure shows the storage tank with LH₂ which is heated by a vaporiser heat exchanger where the cold is recovered for the space cooling system. The vaporised hydrogen is supplied to the PEMFC which produces electricity for the battery, propulsion, auxiliary electricity, and electric boiler. The battery is connected such that it can also supply electricity when discharging. The PEMFC stack is cooled with the heat energy recovery circuit, which provides heat to the hot water system. Any heating loads not covered by the thermal energy recovery is provided by the electric boiler which is connected in parallel.

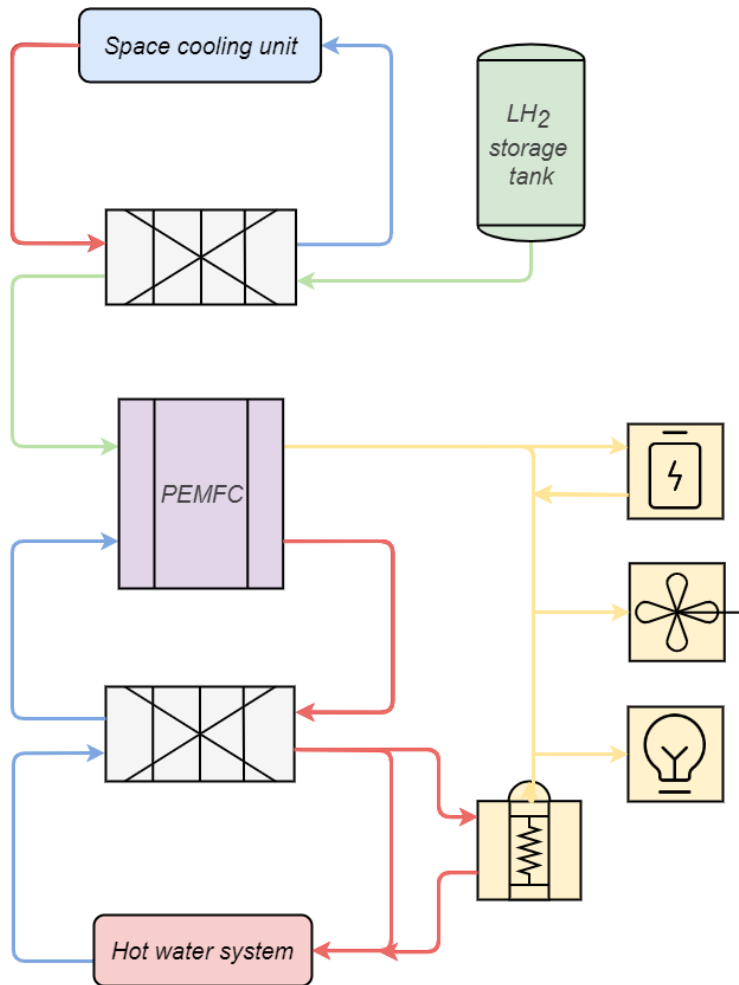


Figure 6: Diagram of FC stack cooling system. Created with diagrams.net.

When determining the capacities of the PEM fuel cell, numbers from the reference case and literature study are applied. It is assumed that the hydrogen fuel cell should cover 80% of the maximum power load, while the battery covers the remaining 20%. The HFC efficiency is estimated at 50%, which is a moderate estimate based on the literature study, and the FC stack cooling load, or recoverable heat energy, of 36% of the input fuel energy is based on the Sankey diagram in Section 2.4. The original gas boilers have an efficiency of 80%, while new electric boilers generally are assumed to reach efficiencies of close to 100%. The original cooler had an EER of 3.5, which corresponds to a COP of 1.03 when using the conversion factor in Equation 1. A new heat pump can be assumed to reach a COP of 4 or 5.

3.1.2 Power Demand

The power demands of the cruise ship for an average day, including for propulsion, auxiliary energy, water and space heating, and space cooling, are all based on the reference case data. To determine the annual energy demands, the duration of each season is necessary. This can be estimated based on the ambient temperatures during a typical year in Sweden. The estimations performed by Ancona et al. [10] is that spring and fall combined last 121 days, summer 62 days, and winter 182 days. The winter scenario is thus evaluated as three times the duration as summer, which is due to the general cold climate in Sweden.

The peak power demand of the energy system determines its design capacity. The necessary installed power will be reduced when introducing energy recovery measures, and three different cases will be used to determine how much the capacity, and therefore also the corresponding installed costs, can be reduced. These cases are also applied to fuel consumption minimisation. Since the energy demand will be reduced, so will the fuel demand and thus also the necessary amount of fuel stored on board of the ship each day. This will decrease the corresponding fuel costs and fuel storage costs.

When optimising the energy production system on board the cruise ship, the reference case will be used for calculations for an easier evaluation of different scenarios. Data from Tables 1 and 5 are used to determine the maximum capacity necessary for the system without any additional measures like thermal energy recovery and storage. The maximum combined power demand peak is obtained by combining the mechanical, auxiliary, and winter space heating power demands for each hour of the day. The average power demands for each case can also be calculated for a better understanding of the power needed, and based on this, the total energy demand for a typical day of operation for each case can be calculated.

Three cases are described to help evaluate the implementation of thermal recovery and thermal storage. The cases are defined below. The base case is the data from the reference case applied to a fully electrical cruise ships driven by a fuel cell. The heating demand is exclusively met with electrical boilers with 100% efficiency and the cooling demand with a chiller with COP of 1.

1. BC (Base Case): The fuel cell and battery system covers all power demands through providing electricity to the different systems.
2. TER (Thermal Energy Recovery): The same as BC, except thermal energy recovery from the system is included.
3. TES (Thermal Energy Storage): The same as TER, except thermal energy storage is also included.

3.1.3 Fuel Consumption

The fuel mass flow rate during one hour is calculated using the HHV of LH₂, the fuel cell electrical efficiency, and the electrical power demand during that same hour. Equation 3 is based on this and also includes two numbers for converting to the correct units. The electrical power demand (P) during one hour is converted from kWh to MJ through multiplication with 3.6. It is then divided by the fuel cell electrical efficiency (η_{FC}), which is 50%, to find the fuel energy needed, and with the higher heating value of LH₂ (HHV), which is 141.7 MJ per kg, which gives the amount of energy per mass in the fuel. To convert the mass flow from kg per hour to kg per second, the number is divided by 3600. The equation is then simplified.

$$\dot{m} = \frac{P \cdot 3.6}{\eta_{FC} \cdot HHV \cdot 3600} = \frac{P}{\eta_{FC} \cdot HHV \cdot 1000} \quad (3)$$

The fuel weight and volume are also calculated based on the fuel demand for 24 hours for each scenario, and for one year. To find the volume of the fuel, the LH₂ density of 0.071 kg per L can be used. For the heating demand, the thermal efficiency of the fuel cell is also included for calculating the fuel demand. Assuming the cruise ship refuels once per 24 hours, the maximum daily fuel consumption determines the storage capacity needed. This can be calculated in terms of weight and volume and should be minimised to reduce costs. A security margin should also be included for safety purposes. The scenario which results in the highest values will be used since the cruise ship must be designed such that it can operate during the entire year.

3.1.4 Thermal Energy Recovery Method

The thermal energy recovery (TER) for the system is based on the numbers from Sections 2.4 and 2.5. However, when calculating the system capacity, it is simpler to have a thermal energy recovery percentage based on the electrical output of the fuel cell instead of the fuel mass flow and its LHV or HHV. Two conversion factors are therefore determined below, one for cold TER and one for hot TER.

For cold energy recovery ratio conversion, Equation 4 is used. The cold energy recovery to electrical energy production ratio (ϕ_{CE}) is the amount of cold energy recovered (CE) to electrical energy produced (EE). The cold energy recovered is determined as 3.2% of the fuel's LHV, which when multiplied with the fuel mass flow gives the cold energy. The electrical energy production is calculated with the fuel cell electrical efficiency (η_{FC}),

which is based on the fuel's HHV. Multiplying this with the fuel mass flow gives the energy produced. Equation 4 is thus created after algebraic simplifications.

$$\phi_{CE} = \frac{CE}{EE} = \frac{0.032 \cdot LHV \cdot \dot{m}_{fuel}}{\eta_{FC} \cdot HHV \cdot \dot{m}_{fuel}} = \frac{0.032 \cdot LHV}{\eta_{FC} \cdot HHV} \quad (4)$$

The same type of reasoning is applied to heat energy recover and results in Equation 5. Here ϕ_{HE} is the heat energy recovery to electrical energy production ratio and HE is the amount of heat energy recovered.

$$\phi_{HE} = \frac{HE}{EE} = \frac{0.36 \cdot HHV \cdot \dot{m}_{fuel}}{\eta_{FC} \cdot HHV \cdot \dot{m}_{fuel}} = \frac{0.36}{\eta_{FC}} \quad (5)$$

The recovered thermal energy is estimated for each hour of a typical day for the reference cruise ship, based on the numbers in Table 1. When no thermal storage is included, it is assumed that the recovered thermal energy for one hour will be used to cover as much of the thermal demand for that hour as possible. Any excess energy will be discarded. Any remaining heat energy demand will be covered by electric boilers, while remaining cold demand is covered by a CO₂ refrigeration heat pump, both based on electricity provided by the fuel cell and battery system. The energy savings from thermal recovery is therefore not purely based on the electricity production, but also on the dynamic thermal demand. However, the total thermal energy that can be recovered will also be presented, as this might be used for other purposes than covering the current thermal demands of the cruise ship.

If there is not enough recovered thermal energy to cover the daily demand, the fuel cell must produce additional electricity for the electric boilers to cover the remaining demand. When no thermal storage is used, and the battery is excluded, the fuel cell must produce the needed electricity for the boilers whenever there is a thermal energy deficit. It is assumed the electrical boilers have an efficiency of 100%. In addition, 36% of the fuel energy consumed by the fuel cell is converted to recoverable heat energy. The energy needed to cover the heat demand can therefore be divided by 1.72 to find the power that must be produced by the fuel cell, giving the total fuel cell production necessary per hour when combined.

The method for calculating the regasification energy, or cold energy, recovery from LH₂ corresponds to the one used to calculate cold recovery potential for LNG. The numbers from Section 2.5 says that LNG cold recovery potential is 1.7% of its LHV, which is 48.6 MJ per kg, meaning that the potential cold energy recovery is approximately 826 kJ per kg LNG. This is close to the minimum amount presented by other articles, meaning that the method should be reliable for calculating a minimum value. Thus, the cold recovery potential of LH₂ will be based on the 3.2% of its LHV of 120 MJ per kg fuel.

3.1.5 Thermal Energy Storage Method

The thermal energy storage (TES) capacity is primarily determined based on calculated in Excel. It is based on the energy demands for the reference case and the recovered thermal energy calculated for this thesis. For every hour where the thermal recovery is higher than the demand, the excess energy production is added to the storage. For hours where the demand exceeds the recovered energy, the thermal storage is discharged accordingly. If the total daily heating energy demand is higher than the total heat energy recovered, the fuel cell must produce the additional electricity needed for the electrical boilers.

Since TES is included, the fuel cell does not need to produce additional electricity for the thermal demand exactly when the demand occurs. Instead, it can be produced at the most convenient time and stored in the TES tank. Although this would lead to additional losses because of heat loss from the storage tank, it could highly benefit the energy production system. There are two different factors that should be considered when deciding when to overproduce. First, the overproduction can smooth out rapid declines in the power demand with the result of a more optimal operation of the fuel cell and maximisation of its lifetime. Second, the thermal storage capacity should be reduced as much as possible to reduce the investment costs for TES. This is achieved by not overproducing when the storage has reached a certain maximum capacity, but only when it is (partly) discharged. Ideally, the hours where the additional energy is necessary coincides with the hours with rapid change, which means the storage capacity can be reduced in addition to smoother fuel cell operation. This decision must be made while also considering the battery contribution to peak shaving.

The storage capacity must be large enough to hold the largest excess thermal energy demand after thermal energy recovery to avoid wasting any recovered thermal energy. This will be calculated by looking at the consecutive hours of thermal energy excess from TER and combining the energy recovered for these hours. The TES should be discharged at the first opportunity after charging to optimise the fuel cell operation, and then charged again when possible. This can be done as often as needed based on the demand curve.

The thermal energy storage capacity and design is determined separately for each of the three cases (BC, TER, and TES). The season with the highest capacity necessary will be used as the overall design, since only one design for the cruise ship will be used for the entire year. However, results for all scenarios will be presented since it provides a broader application area for future work when including a range of ambient temperatures.

3.1.6 Battery Implementation

A battery is to be implemented into the energy provision system. This is primarily done to reduce the fuel cell capacity, optimise its operation and maximise its lifetime, as described in Section 2.6. For simplicity, it is assumed the battery should be able to cover 20% of the highest power demand. The fuel cell capacity should be reduced accordingly. Since the installed capacity is designed based on the scenario with the highest power peak, the battery capacity should be designed based on the same assumption.

When reducing the fuel cell capacity, the recoverable heat energy potential will also be reduced accordingly since the fuel cell production is reduced when the battery discharges. However, the fuel cell system will at one point recharge the battery, increasing its production again during times of low power demand. For when TES is included, the net thermal energy recovery will thus be the same. The battery will also produce heat which must be removed and may be recovered as well. For simplicity, it is therefore assumed that the total thermal energy recovery is constant regardless of battery implementation.

3.2 Dynamic Calculations

The hot and cold thermal energy recovery was also evaluated with dynamic calculations by simulating the proposed systems. This was done with the programming language Modelica which was used in the dynamic modelling software Dymola. Components from the TIL library were included. The models were made separately for easier implementation and evaluation of the results. They include a heat energy recover model and a few cold energy recovery models with varying complexity.

3.2.1 Heat Energy Recovery Simulation

The heat energy recover model in Modelica simulates the recovery of heat produced by the fuel cell system, used to fill the hot water demand of the cruise ship. It should therefore include a representation of the fuel cell stack producing a heat flow dependent on the electricity production, and water circuits which recover this heat. The finished model is presented in Figure 7. A model with only one heat exchanger was also created and can be found in Figure 40 in the appendix. The model will be explained in detail in the remainder of this section.

The fuel cell stack is represented by a tube with a heat flow applied to it. The heat flow load should correspond to the recoverable heat produced by the fuel cell, as described in Section 3.1.4. The model reads an CSV file where the heat loads and time steps are listed. The time interval for the model is 1000 seconds, while the heat production profile is based on 24 hours with one heat power value per hour. Therefore, the 1000 interval is divided into 24 steps to be able to simulate the full profile. The change in load between the time marks is assumed linear.

The function of the main circuit is to regulate the temperature of the fuel cell stack. The coolant is circulated with a simple hydraulic pump, which is regulated by the exit temperature of the fuel cell stack by a PI regulator. The maximum temperature of the fuel cell is assumed to be 200 °C, as it is assumed to be a high temperature PEM fuel cell, and the temperature can vary from this value down to 180 °C to ensure maximum efficiency of the fuel cell. The set point temperature of the FC stack outlet is therefore chosen to be 180 °C to avoid overheating due to slow regulation by the PI controller.

The exiting fluid from the stack is cooled through the first plate heat exchanger, where the water in the secondary circuit is heated. This circuit supplies the HT hot water demand of the ship and should have a temperature of 90 °C. The water mass flow rate is therefore

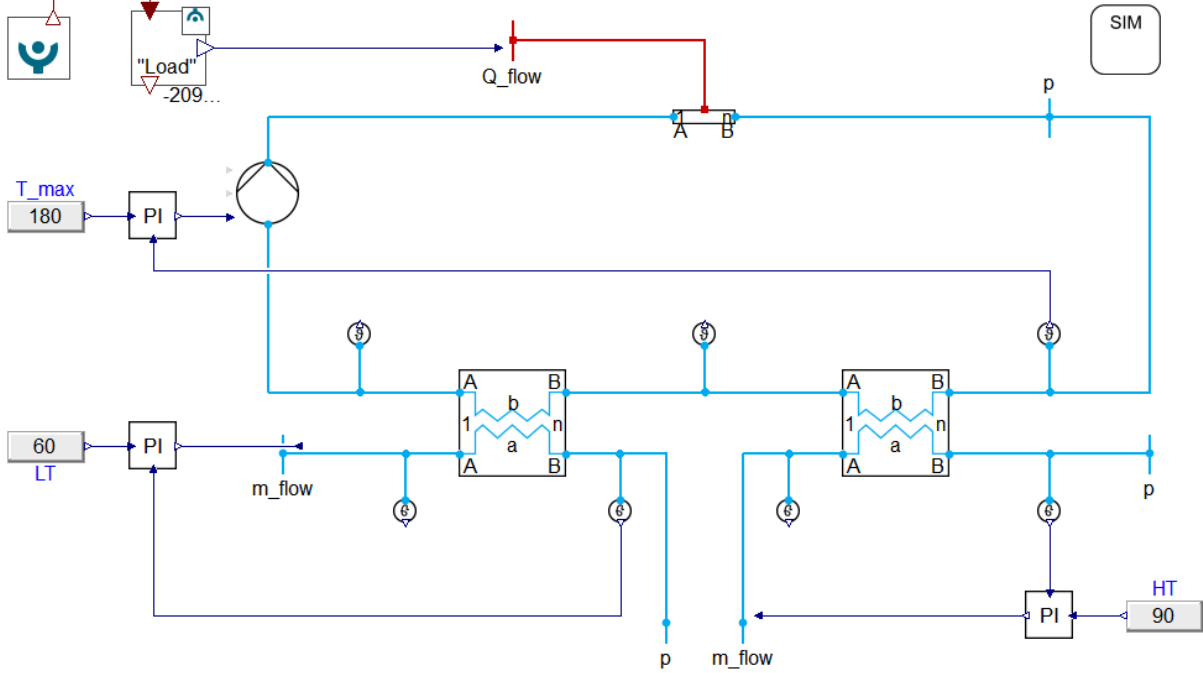


Figure 7: Modelica model of heat energy recovery from hydrogen fuel cell stack.

regulated such that the fuel cell coolant heats it to up to 90 °C. The second plate heat exchanger provides water for LT hot water demand, which is assumed to be 60 °C. It can also be used for thermal storage purposes if the entire hot water demand is covered. The temperature is measured at several places in the model and can be seen in Figure 7. The inlet water flow for the first heat recover circuit is return water from the hotel loads and is assumed to be 25 °C. The second circuit has a inlet water temperature of 10 °C. The pressure in the cooling circuit is kept at 1.013 bar. The temperatures for the different streams are measured using temperature sensors.

The coolant choice is based on the literature presented in Section 2.4 in combination with which liquids are available in Modelica. For the secondary flow, water is chosen as it allows for direct use for the hot water demand from the hotel loads. Based on the further use of the liquid, however, this fluid can be changed to one with more fitting properties like higher boiling point or thermal conductivity. For the coolant circulating through the PEMFC stack, the three different Therminol heat transfer fluids available in Modelica are tested and compared. The ones available are listed in Table 4. A 50:50% volume mix of propylene glycol and water is also available in Modelica and was used for initial testing. For these simulations, the set point temperature for the FC stack outlet had to be lowered from 180 °C to 104 °C to avoid vaporising the coolant.

3.2.2 Cold Energy Recovery Simulation

The cold recovery model cools a working medium through heat exchange with the liquid hydrogen fuelled to the fuel cell. Several different versions were developed and tested. One of them will be presented here, while the remaining models can be found in Appendix A.

All models read a CVS file with the LH2 mass flow rate from the fuel storage tank to the fuel cell. The flow rate is determined as described in Section 3.1.3, based on the hourly electrical power demands of the ship.

The model presented in this section can be seen in Figure 8. The liquid hydrogen is vaporised through heat exchange with the recovery circuit before entering the fuel cell. The "cold energy" can either be recovered directly by a water stream which then supplies cold water to the air conditioning system, providing space cooling for passengers. The second option is supplying it to a CO₂ refrigeration unit which can utilise the energy much more efficiently due to its heat pump characteristics. Due to the time constraints of this project, the CO₂ refrigeration unit was not modelled, so the model in the figure shows a water circuit recovering the cold energy. The cooling water should have a temperature of 5 °C, which is thus the set point in the model, and it is important that this temperature does not drop to 0 °C or below to avoid freezing. A simple pump circulates the stream and is regulated by a PI controller to keep the temperature at 5 °C. A tube represents the space cooling system, and a heat flow boundary is connected to simulate the cooling demand. The cooling demand load from the reference case is provided through a CVS file read by the simulation.

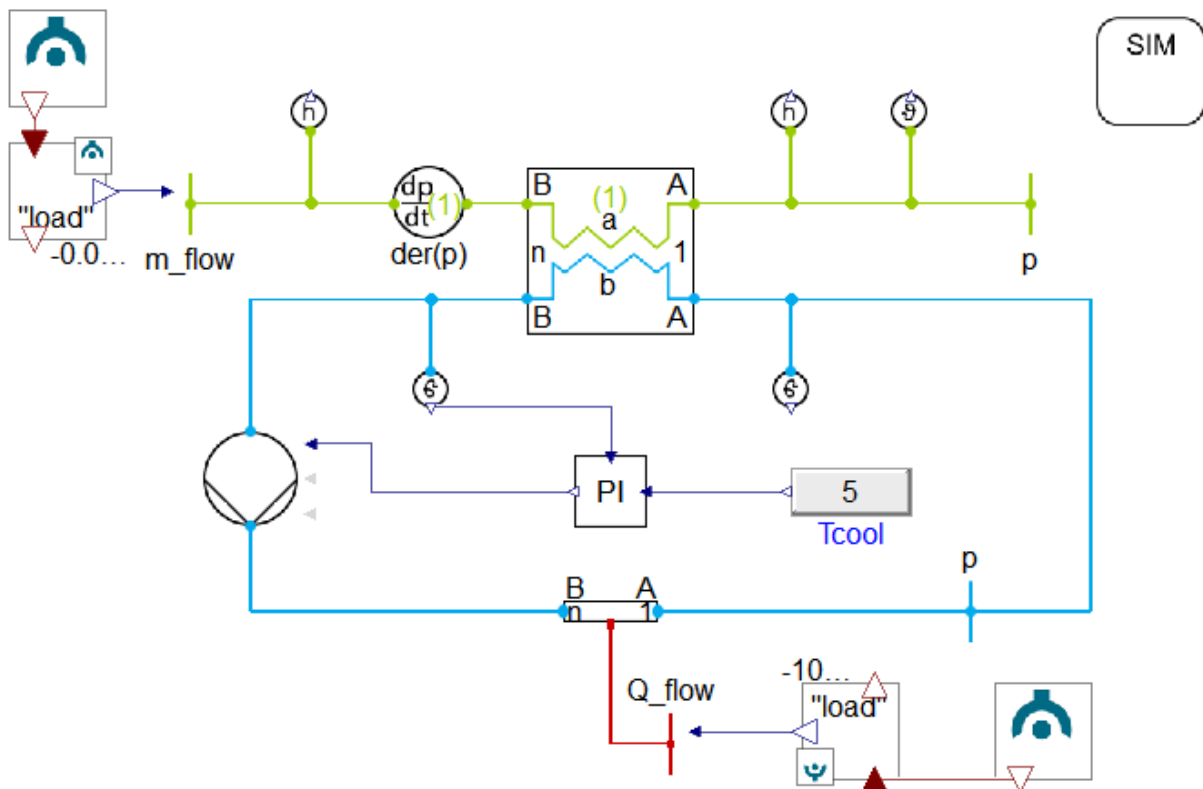


Figure 8: Modelica model of cold energy recovery directly with water.

For a model recovering the cold energy and providing this to the CO₂ refrigeration system, a medium other than water should be used which have a lower freezing point. This will reduce the mass flow rate and thus also necessary pumping power. The PI controller should then regulate the mass flow rate of the secondary stream such that its temperature does not fall below its freezing point. Figure 9 shows such a model, where the secondary stream recovers cold from the hydrogen flow. The CO₂ unit is not included but can be added for future work. For this model, Therminol D-12 is used as its working medium, which has a minimum use temperature of -94 °C, as presented in Section 2.4. The PI controller is set to reach -90 °C.

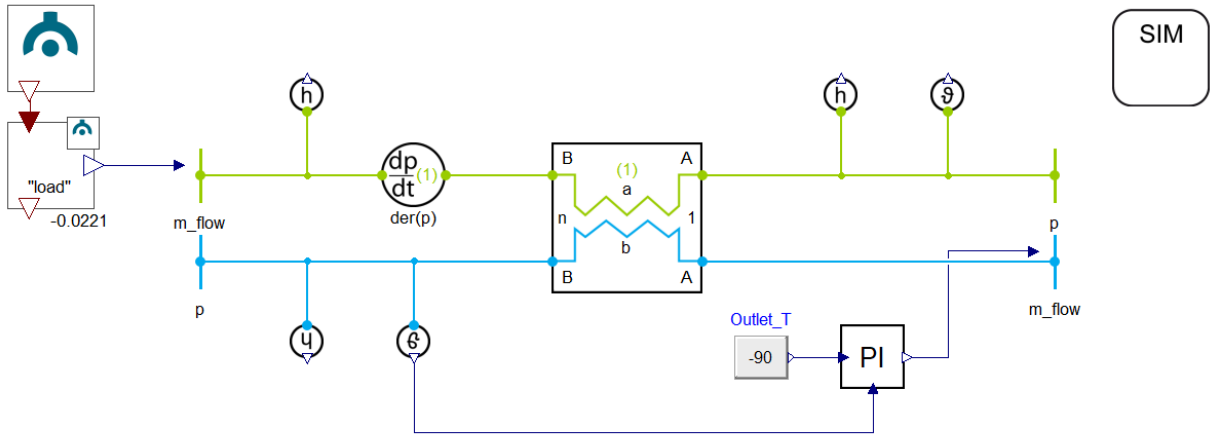


Figure 9: Modelica model of cold energy recovery with secondary stream.

The LH2 must be heated to room temperature before entering the fuel cell, and since the LH2 has very low enthalpy initially, the temperature lift is relatively large. Also due to the mass flow rate, the system will need a heat exchanger system with a large surface area, or alternatively several exchangers. Several exchangers can also be used if the recovered cold energy is used for different purposes. For simplicity, only one exchanger with a larger surface area is used in Modelica.

3.2.3 Combined Recovery Model

The two thermal energy recovery models can also be combined. The recovered heat should cover the heating demand as much as possible, since it has a high temperature. If there is leftover recovered heat energy, however, this can be used for other purposes, such as vaporising the hydrogen fuel. The same is the case for the cold energy recovery, where it should cover the space cooling demand as far as possible. Any remaining heating needed for the hydrogen can be taken from leftover recovered heat. The developed model can be found in Figure 43 in the appendix, but due to time restrictions, it has not been optimised or tested extensively.

4 Results

4.1 Reference Case Energy Demand

The energy system design is based on the energy demands of the reference cruise ship described in Section 2.1. All calculations are based on the data in Table 1, which are plotted in Figure 11. The figure includes summer conditions (11a), spring/fall conditions (11b), and winter conditions (11c). The propulsion and auxiliary electricity demands are assumed constant during the year, while the heating and cooling demands are season dependent.

The combined power demand for each scenario is illustrated in Figure 10. Assuming the boilers have 100% thermal efficiency, the heating demand can be added directly to the other electrical demands. The power peak occurs at 9 am for all seasons. Winter conditions show the continuously highest power demand, while summer and spring/fall conditions switch between showing the second highest and lowest power demands. For the peak at 9 am, summer shows the second highest power demand.

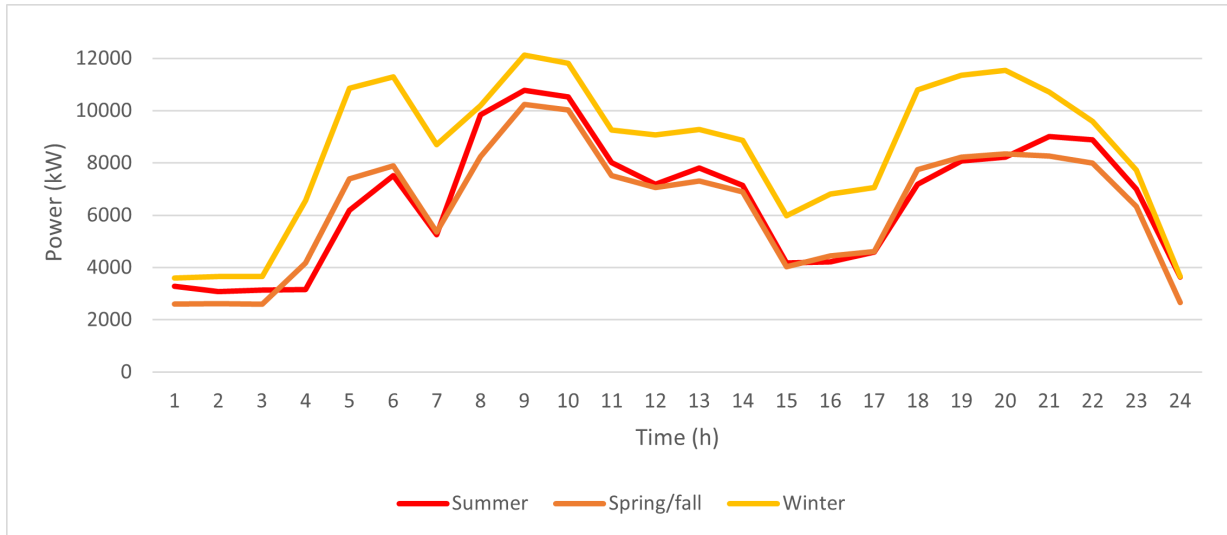
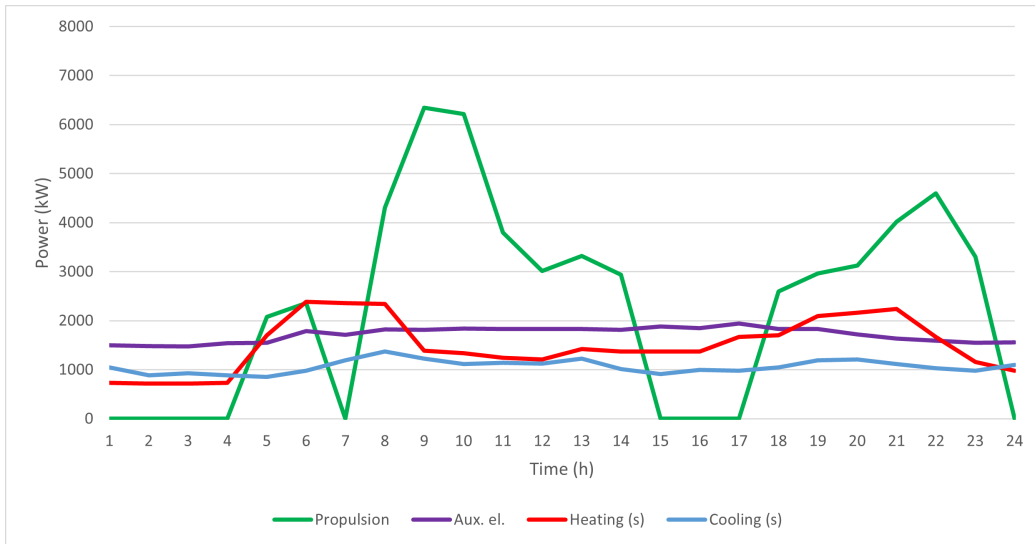
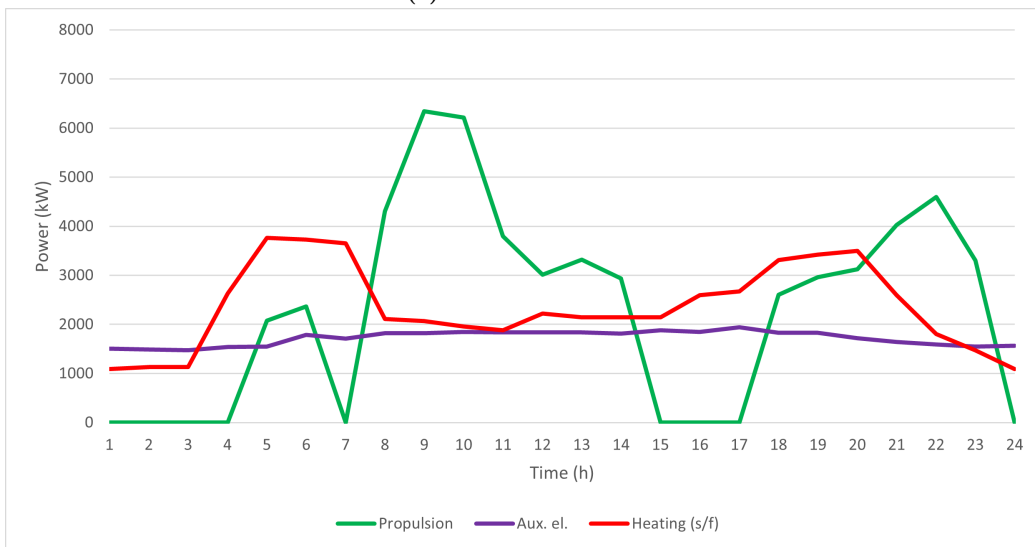


Figure 10: The combined power demand of the cruise ship for all scenarios. Includes propulsion, auxiliary electricity, heating, and cooling for summer.

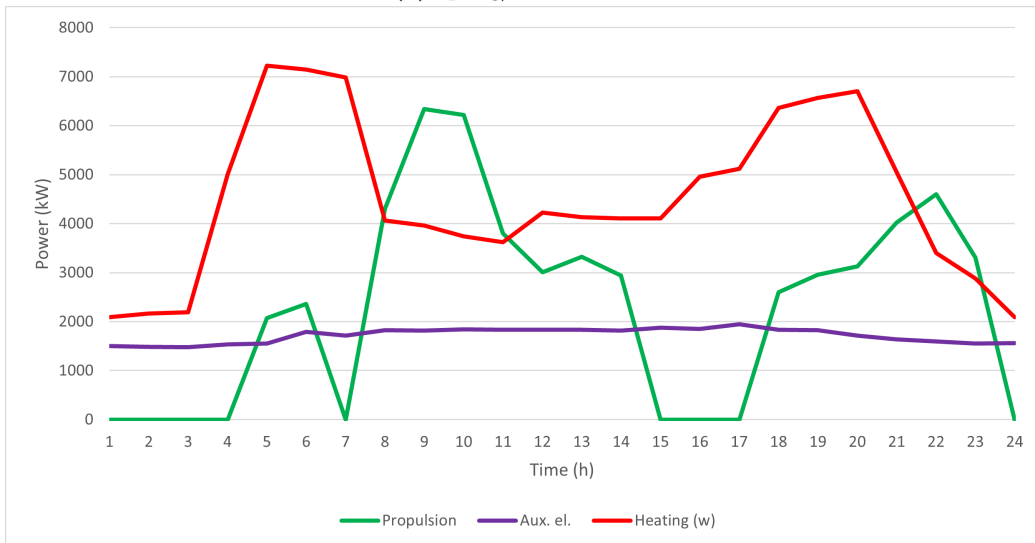
The highest peak occurring for each scenario is presented in Table 5. The maximum power occurs at 9 am, as discovered from Figure 10. The highest possible power demand during the year for the reference cruise ship is therefore 12.13 MW, and happens during winter at 9 am. The average daily power demands are also presented for each scenario in Table 5. For any day during the year, the average power will be 7.466 MW. This is calculated by adjusting the average of each scenario based on their duration.



(a) Summer conditions.



(b) Spring/fall conditions.



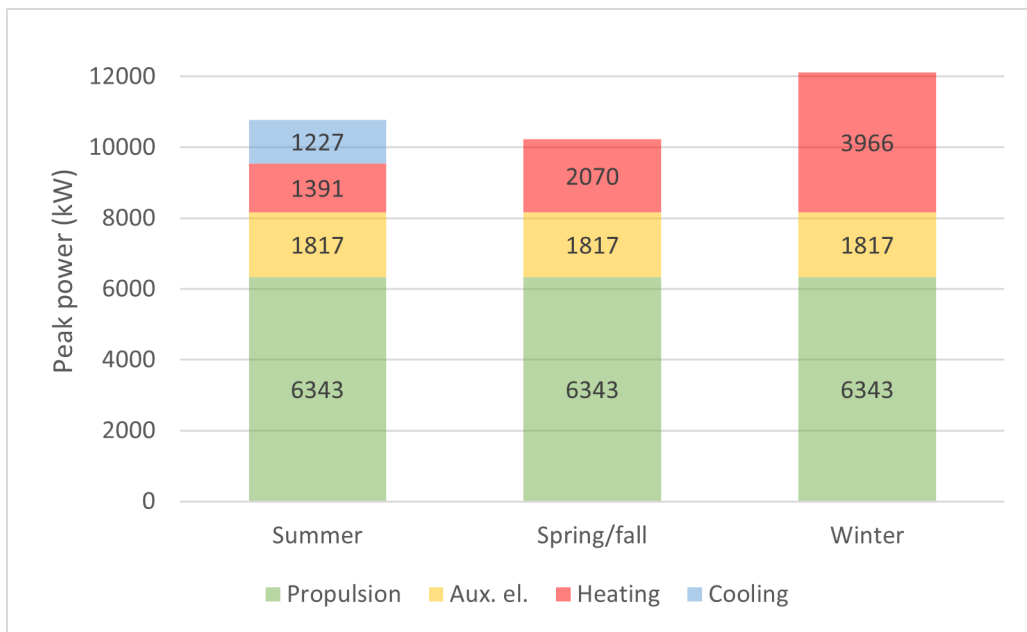
(c) Winter conditions.

Figure 11: Energy demands of the reference cruise ship.

Table 5: Peak and average power demands for all scenarios.

	Max. power [MW]	Average power [MW]
Summer	10.778	6.580
Spring/fall	10.230	6.354
Winter	12.126	8.506

The size of the different power demands at this hour is illustrated in Figure 12. The propulsion and auxiliary electricity demands are constant for all scenarios, the heating demand is largest during winter and smallest during summer, while the cooling demand only occurs during summer. From the figure one can see that the combined power peak is largest during winter conditions and smallest during spring/fall conditions.

**Figure 12:** Power demands at 9 am for all scenarios.

The annual energy demand for the reference cruise ship is calculated with the data from Table 6 and the amount of days that each scenario lasts. As presented in Section 3.1, summer is estimated to last 62 days, fall/spring 121 days, and winter 182 days.

Table 6: Daily energy demand for each scenario and annual energy demand.

	Summer [MWh/d]	Spring/fall [MWh/d]	Winter [MWh/d]	Annual [GWh/y]
Propulsion	54.99	54.99	54.99	20.07
Aux. el.	41.25	41.25	41.25	15.06
Heating	36.11	56.27	107.91	28.69
Cooling	25.57	0	0	1.585
Combined	157.9	152.5	204.1	65.39

4.2 Thermal Energy Recovery

4.2.1 Heat Energy Recovery

The amount of recoverable heat energy per electrical energy produced is calculated with the ratio (ϕ_{HE}) derived in Equation 6. It is based on the electrical efficiency of the fuel cell (η_{FC}) of 50%.

$$\phi_{HE} = \frac{0.032}{\eta_{FC}} = \frac{0.36}{0.50} = 72\% \quad (6)$$

Based on this ratio and the data in Table 1, the amount of recoverable heat energy is calculated for each hour. The resulting recoverable heat is plotted in Figure 13, and the values for each hour can be found in Table 15. The plot also includes the heating demands for summer (s), spring/fall (s/f), and winter (w) conditions for comparison. The recoverable heat is purely based on the electricity production to cover propulsion and auxiliary electricity demands. As these demands are constant for all scenarios, so is the heat energy recover.

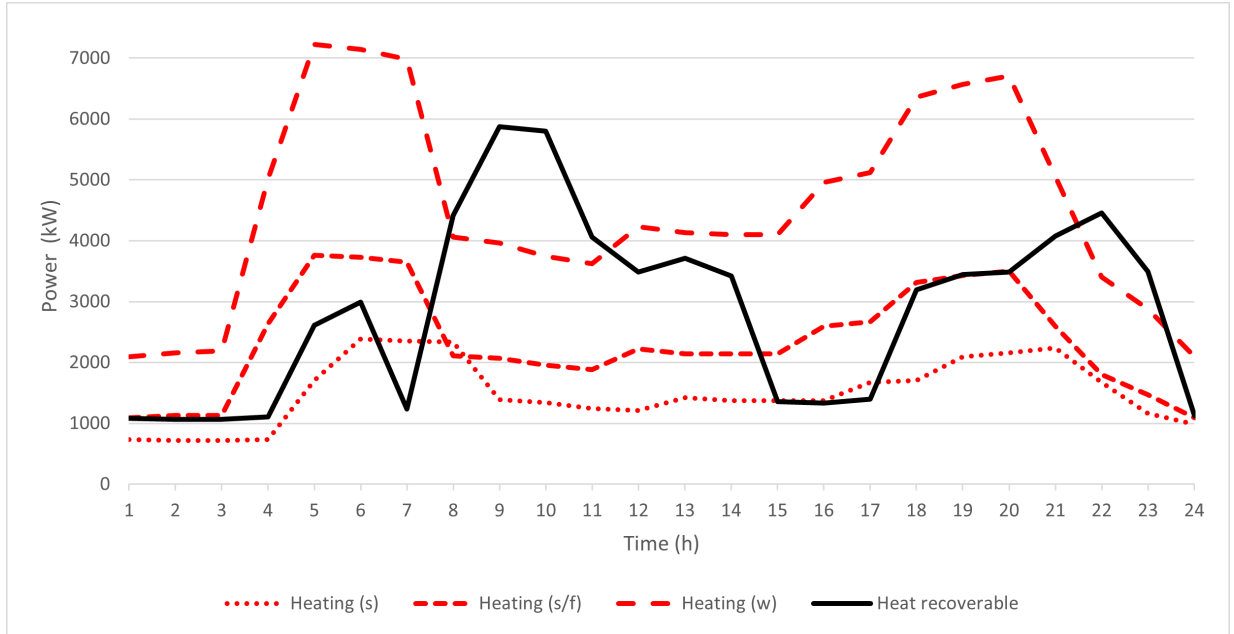


Figure 13: The heating power demand for summer, spring/fall, and winter conditions, and the heat energy that can be recovered during a typical day.

Since the total daily electricity demand of the ship needed for propulsion and auxiliary electricity is 96.24 MWh, as presented in Table 6, the total amount of recoverable heat energy each day is 69.29 MWh. Figure 14 shows that the recoverable heat energy for one day covers the daily demand for summer and spring/fall conditions, but not for winter conditions, where it covers 64%.

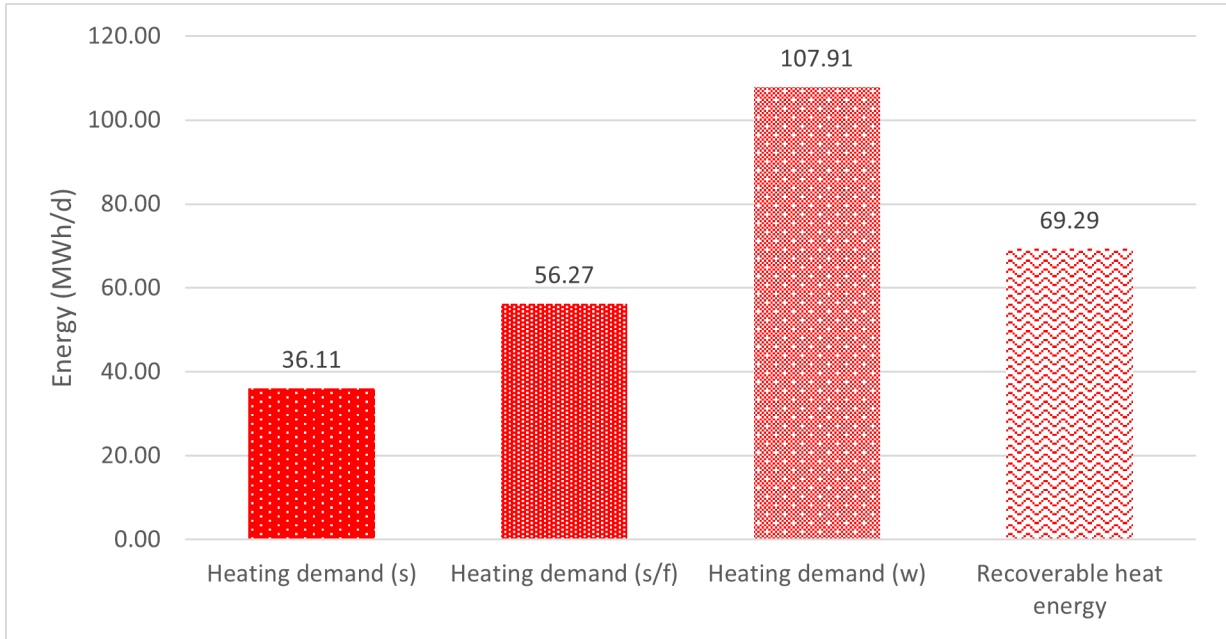


Figure 14: Daily energy demand for each scenario and daily recoverable heat energy.

Without storage, the recovered heat energy is used directly to cover heating demands. The usable recovered heat energy must therefore be calculated hour by hour for one trip. The actual recovered heat energy for one day based on this method is presented in Table 7. From the table one can see that there is leftover heating demand for all scenarios, even though the total daily available heat is larger than the demand for the summer and spring/fall scenarios.

Table 7: Daily heat energy demand for all scenarios and cases.

Energy demand [MWh/d]	Heating demand	Recovered heat	Leftover heating demand
Summer (62 days)	36.11	34.66	1.45
Spring/fall (121 days)	56.27	46.84	9.43
Winter (182)	107.91	62.87	45.04
Annual	286,87	19,259	9,428

When including thermal recovery, the system can recover 5875 kW at 9 am, meaning that the heating demand is completely covered at 9 am. Figure 15 illustrates the reduction in the maximum power peak for the cruise ship. The peak is reduced to 8160 kW, which is a reduction of 32.71%.

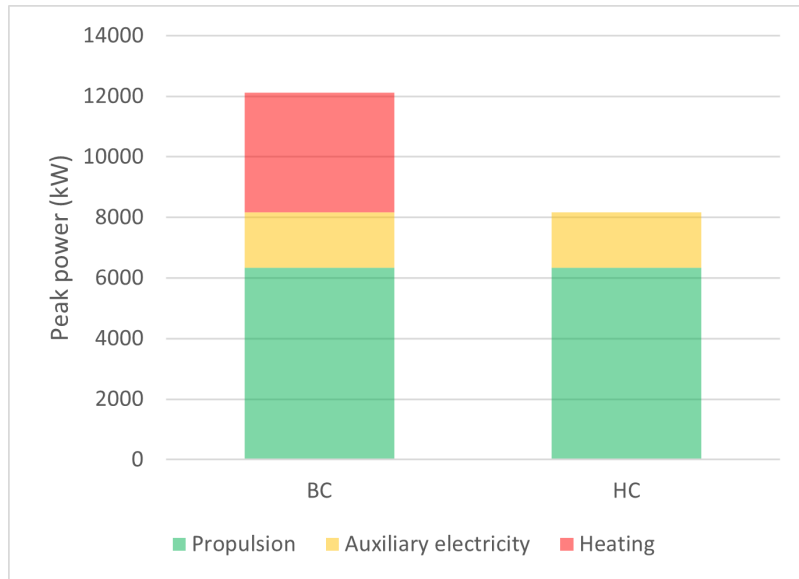


Figure 15: Power demands at 9 am for all scenarios.

The remaining heating demand is covered by the electric boilers. From Figure 13, one can see that the heating deficit happens at 7 am and 3 pm to 5 pm for the summer scenario. For spring/fall, it happens at 1 am to 7 am, 3 pm to 6 pm, and at 8 pm. For the winter scenario, it lasts from midnight to 7 am and from 12 am to 9 pm. The total electricity demand when including the remaining heating demand is illustrated in Figure 16. All three scenarios are included. For summer and spring/fall conditions, the total electricity demand is a little higher than when only looking at the propulsion and auxiliary electricity demands, while for winter conditions, the demand is higher for most of the hours. The power peak at 9 am, which is identical for all scenarios, is not affected by the additional production. The overall daily electricity production, however, increases.

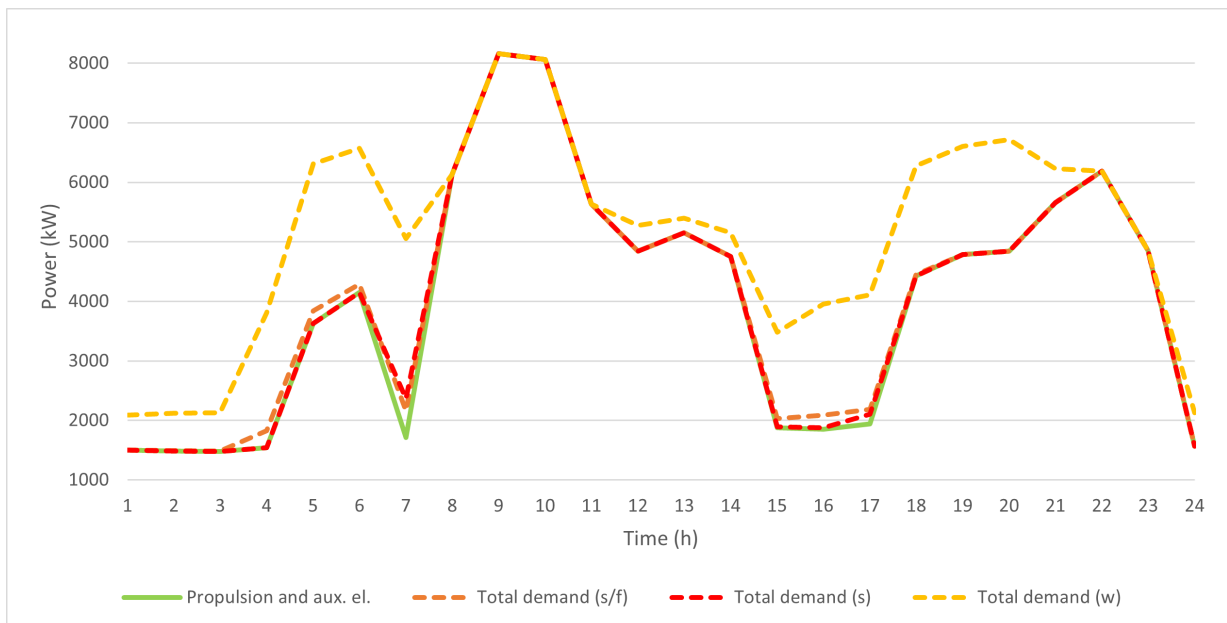


Figure 16: Total power demand for all summer, spring/fall, and winter scenario when no thermal energy storage is used.

4.2.2 Cold Energy Recovery

The recoverable cold energy is determined with the ratio calculated in Equation 7.

$$\phi_{CE} = \frac{0.032 \cdot LHV}{\eta_{FC} \cdot HHV} = \frac{0.032 \cdot 120.0MJ}{0.50 \cdot 141.7MJ} = 5.42\% \quad (7)$$

The cold energy which can be recovered during a typical day (cold energy available) is plotted in Figure 17. This amount divided by 5 is also plotted (cooling provided), to account to the refrigeration unit with COP of 5. The cooling demand is also included for comparison. For the recoverable cold energy, the demand is higher at all times during the day, with the graph only applying to summer conditions as there is no cooling demand for the other seasons.

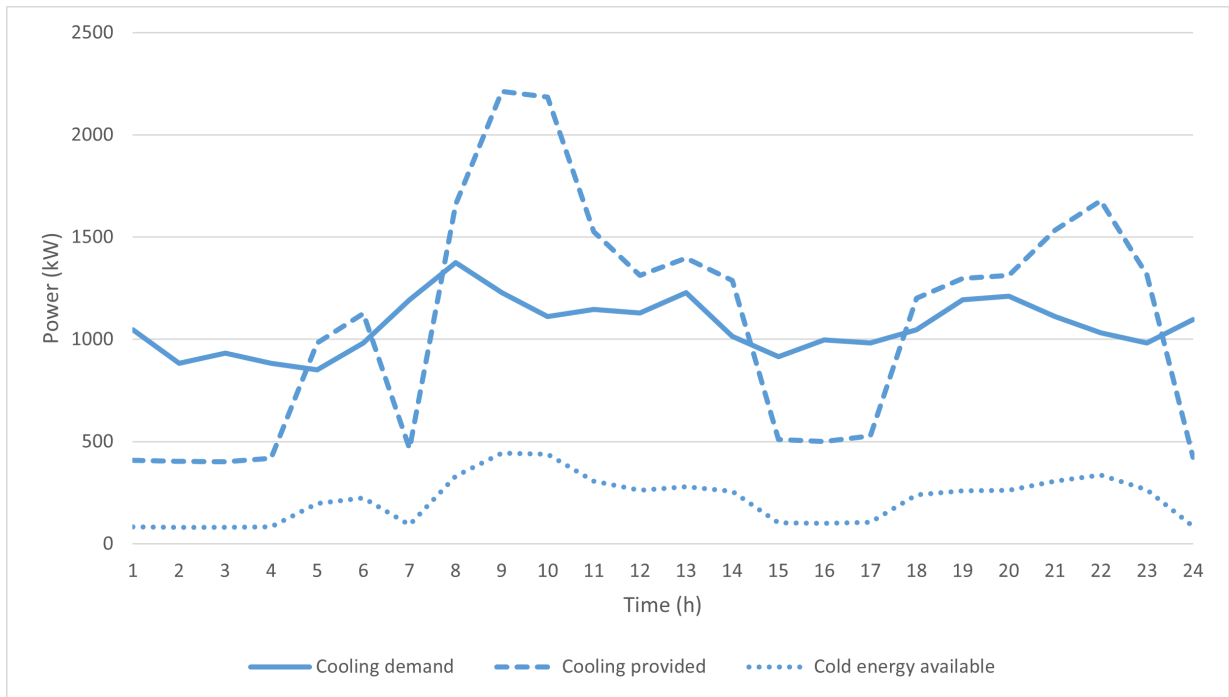


Figure 17: Cooling demand, cold energy that can be recovered, and the cooling power from a heat pump with COP = 5.

The total amount of available cold energy and the cooling demand are illustrated in Figure 18. The total daily recovered energy exceeds the energy demand. They are both only applicable to summer conditions.

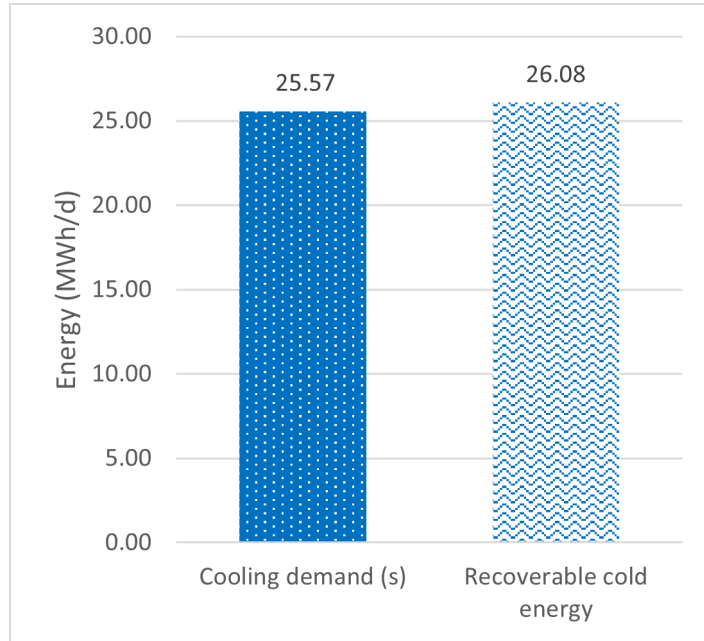


Figure 18: Daily available recoverable cold energy and the daily space cooling demand.

4.3 Thermal Energy Storage

Including thermal storage has no effect on the maximum power demand. This is because the thermal recovery covers the entire demand. However, both heat and cold energy storage reduces the cruise ship’s fuel consumption.

4.3.1 Heat energy storage

The recovered heat energy not used directly to cover heating demand is stored in hot water tanks with a temperature of 90 °C.

When including heat storage, all of the recovered heat energy can be utilised, whereas when not included, there is leftover heating demand for all scenarios, as was presented in Table 8.

Table 8: Daily heat energy demand for all scenarios and cases.

Energy demand [MWh/d]	Heating demand	Recovered heat	Leftover heating demand
Summer (62 days)	36.11	36.11	0
Spring/fall (121)	56.27	56.27	0
Winter (182)	107.91	69.29	38.62
Annual	28,687	21,658	7,029

The heating demand during the whole day for winter condition is illustrated in Figure 19. The BC shows the actual heating demand of the cruise ship. The TER case shows the remaining heating demand after the recovered heat energy has been used, while TES shows

how much is left when heat storage is included. For the TES case, the demand curve can be changed based on when the heat storage is charged and discharged, based on the fuel cell load.

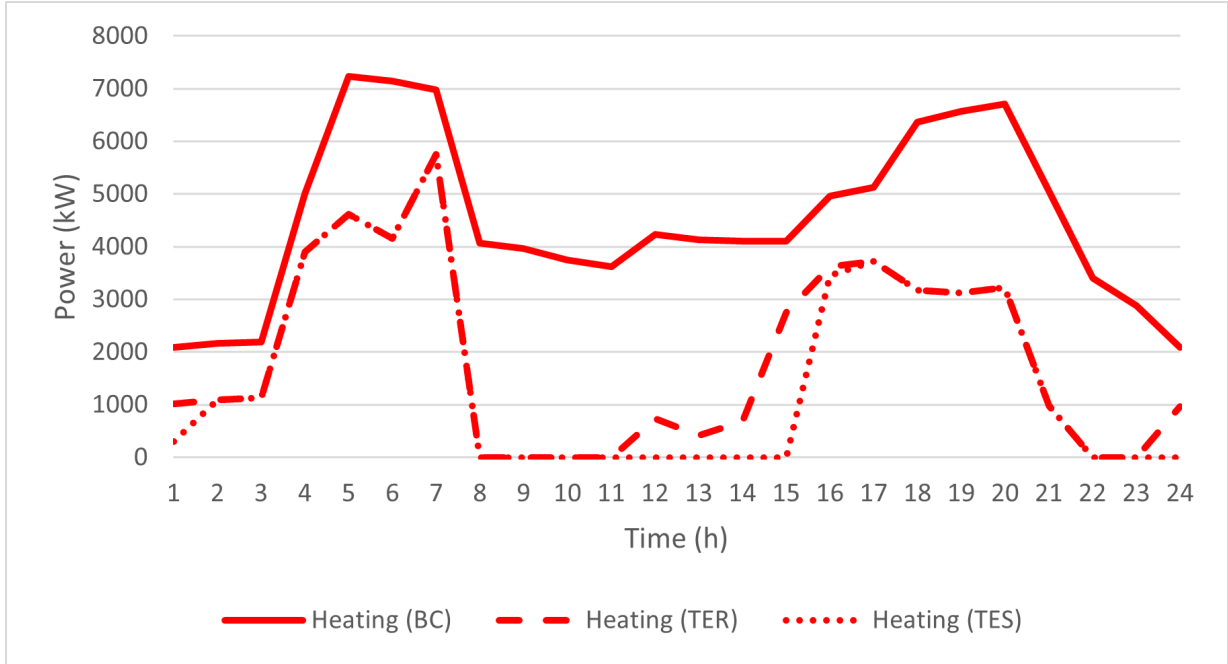


Figure 19: Maximum heating demand for all cases.

4.3.2 Cold Energy Storage

When assuming a CO₂ refrigeration heat pump with a COP of 5, the entire cooling demand can be covered with cold recovery. However, as with hot thermal energy recovery, there are times during the day where the recovered cold either does not fully cover or exceeds the cooling demand. Storage is therefore necessary to utilise the full cold TER.

The daily and annual cooling demand for the base case and when including TER and TES are presented in Table 9.

Table 9: Daily and annual cooling demand for all cases

	BC	TER	TES
Daily cooling demand [MWh/d]	25.57	4.880	0
Annual cooling demand [MWh/y]	1585	303.6	0

4.4 Fuel Demand Evaluation

The fuel consumption of the cruise ship is based on the electricity demand on the cruise ship and the fuel cell system efficiency. All energy demands are met through electricity or thermal recovery. Therefore, the energy demands of the cruise ship is first presented, with and without thermal recovery and storage. The annual values are based on the data for each season and the duration of each season.

The daily energy demands of the cruise ship for all cases are presented in Table 10. The propulsion and auxiliary electricity demands are combined as "Prop + aux". The energy demand is reduced when including TER and completely covered with TES, except for heating demand during winter conditions.

Table 10: The daily energy demands for each scenario.

Daily energy demand [MWh]	BC	TER	TES
Prop + aux	96.24	96.24	96.24
Heating (s)	36.11	1.454	0
Heating (s/f)	56.27	9.430	0
Heating (w)	107.9	45.05	38.62
Cooling (s)	25.57	4.880	0

The annual energy demands of the cruise ship for all cases are presented in Table 11. It is based on the data in Table 10 assuming summer lasts 62 days, spring/fall 121 days, and winter 182 days.

Table 11: Annual energy demands for the different energy categories for all three cases.

Annual energy demand [GWh]	BC	TER	TES
Prop + aux	35.13	35.13	35.13
Heating	28.69	9.429	7.028
Cooling	1.585	0.303	0
Total	65.40	44.86	42.16

The daily and annual fuel consumption for all scenarios and cases is presented in Table 12. The different properties demanding energy are combined into the total fuel demand. It is assumed that the CO₂ refrigeration system is implemented such that the space cooling demand can be met with less energy than it provides due to its COP of 5. For heating, the electric boilers are assumed to have 100% efficiency.

Table 12: Daily fuel consumption for each scenario and fuel consumption for the whole year, for all cases.

Fuel consumption	BC	TER	TES
Summer [kg/d]	6,985	5,014	4,890
Spring/fall [kg/d]	7,749	5,369	4,890
Winter [kg/d]	10,373	7,179	6,852
Annual [tonne/y]	3,245	2,267	2,142

The maximum daily fuel consumption for all cases is for the winter scenario, which thus corresponds to the fuel storage capacity needed for the cruise ship. The reductions in percentages based on the BC when including TER and TES are presented in Table 13. The maximum power needed is not affected by TES as all thermal energy demand is covered through recovery. Thus, the systems capacity is only affected by TER. This is also

included in the figure based on Figure 15. The effect of TER and TES is also visualised in Figure 20.

Table 13: The reduction of annual fuel consumption, fuel storage capacity, and energy system capacity when including TER and TES.

Reduction compared to BC	TER	TES
Annual fuel consumption	30.05%	33.75%
Fuel storage capacity	30.79%	33.94%
Energy system capacity	32.71%	32.71%



Figure 20: The effect of including TER and TES on annual fuel consumption, fuel storage capacity, and energy system capacity.

4.5 Battery Influence on System

The implementation of a battery in the energy system affects the fuel consumption, storage capacity and the needed fuel cell installed power. These factors are reduced proportionally to the installed power of the battery. The fuel cell production curve is also affected, depending on when the battery is discharged and charged. This can be determined based on the electricity demand curve with the goal of smoothing out the curve through load shifting.

One option tested is fully discharging the battery during the highest power demand peak and charging it through the following valleys. The original power curve is the total power demand from the fuel cell and battery system when TER and TES are included. The curve is altered when using the battery to smooth it out. The peak power demand for the fuel cell is originally 8160 kW. The battery is applied such that the peak is reduced, which is done both for 9 am and 10 am. It is adjusted such that the new peak occurs both at 9 am and 10 pm. The new power peak is 7295 kW. This is a reduction of 10.6%.

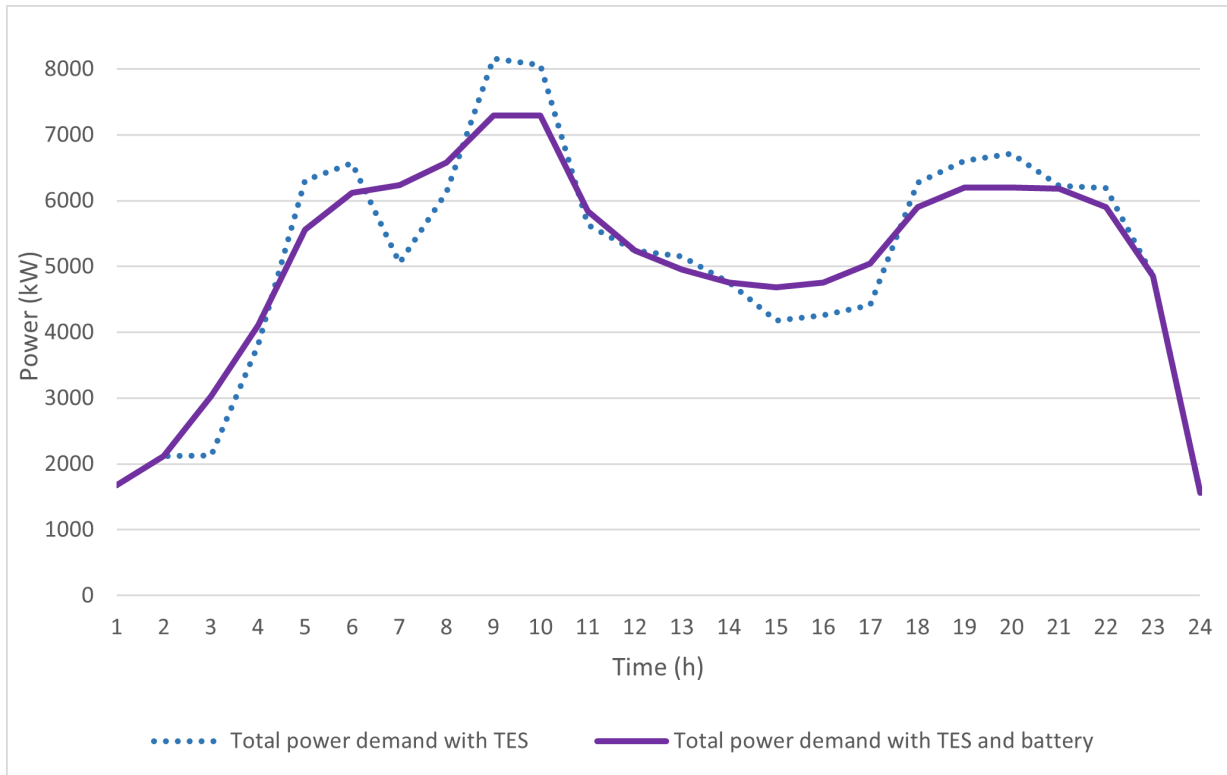


Figure 21: Total power demand with peak shifting from battery implementation.

4.6 Dynamic Calculations

In this section, the simulation results from Modelica are presented. They include coolant testing as well as results from two different models, which represent the heat and cold energy recovery circuits. Extended models can be found in Appendix A.

4.6.1 Coolant Comparison

Five different working fluids for the heat energy recover circuit were used in early stage simulations and compared in terms of mass flow generated. The model used for testing is similar to the final heat energy recover model, except with a single secondary circuit instead of two. Figure 40 in Appendix A shows this model. The heat flow load profile applied to this model is presented in Table 14. The coolants tested were Therminol 66, Therminol 59, Therminol D-12, a 50:50% water and propylene glycol mixture, and pure water.

Table 14: The heat flow load profile for the coolant testing.

Time [s]	Load [kW]
0	4608
300	4608
400	3917
600	3917
1000	922

The flow rates for both the cooling circuit stream and the secondary stream were measured with each of the Therminol coolants. The recovery water stream mass flow is identical for all three coolants. From Figure 22 one can see that Therminol D-12 resulted in the lowest mass flow rate and Therminol 66 gave the highest, leaving Therminol 59 in the middle.

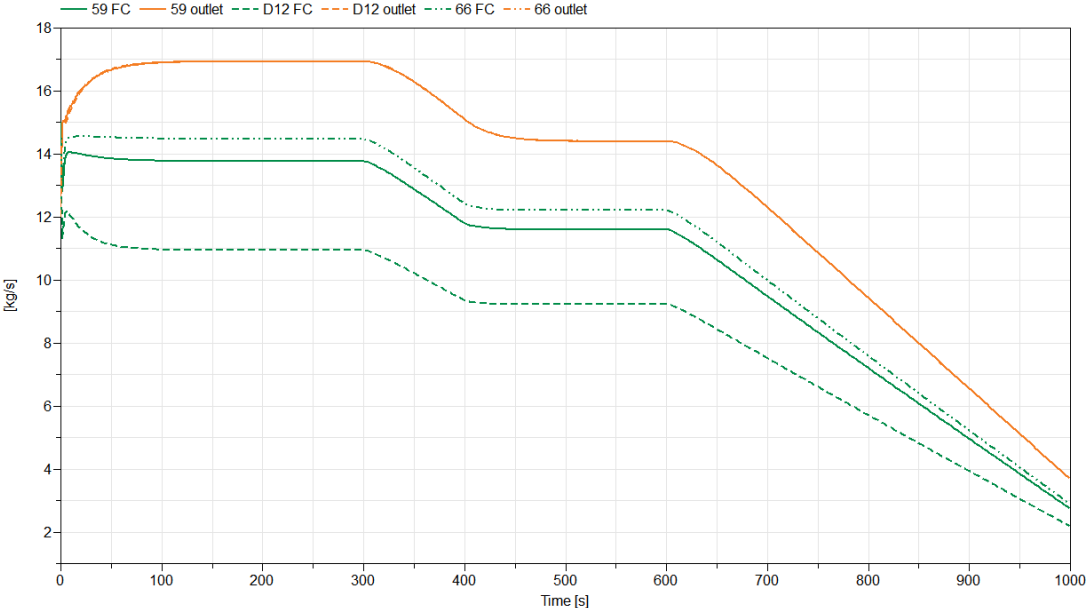


Figure 22: Cooling circuit and secondary stream mass flow rates for three coolants.

Simulations were also performed using pure water and a 50:50% water and propylene glycol mixture. The outlet temperature was set to 80 °C. Figure 23 shows the resulting mass flow rates for both coolants. The outlet flow rate was unchanged from the simulations using Therminol, but the coolant circuit flow rates increased drastically and hit the upper limit of 30 kg per second also for average FC cooling load.

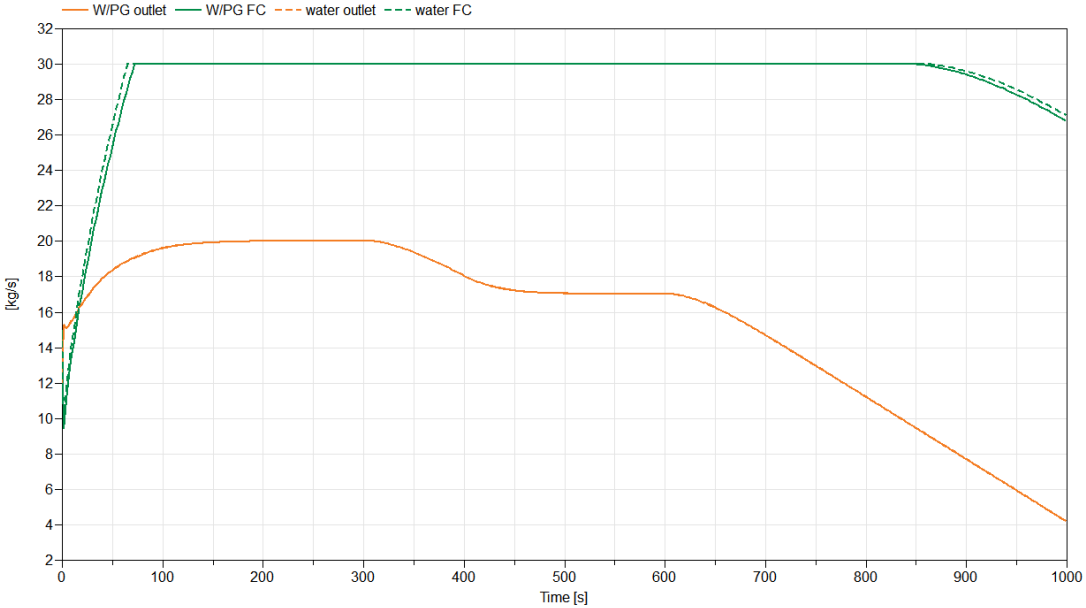


Figure 23: Cooling circuit and secondary stream mass flow rates for water and PG/W.

Since the Therminol D-12 coolant resulted in the lowest mass flow rate, this was used for the remainder of the Modelica simulations, including both the heat and cold energy recovery models.

4.6.2 Heat Energy Recovery Model

The results from the heat energy recovery model produced in Modelica, which was shown in Figure 7, are presented in this section. The heat flow load profile applied to the simulated fuel cell stack is presented in Table 15 and is based on a time interval of 1000 seconds, as explained in Section 3.2.1.

Table 15: The heat flow loads applied to the simulated fuel cell stack.

Time [s]	Heat flow [kW]
0	1125
42	1081
83	1069
125	1063
167	1109
208	2611
250	2990
292	1233
333	4413
375	5875
417	5805
458	4057
500	3489
542	3711
583	3424
625	1354
667	1331
708	1400
750	3190
792	3448
833	3486
875	4076
917	4458
958	3493
1000	1125

When running the model, the resulting values at 375 seconds, which is when the heat production is the highest, are displayed in Figure 24. The temperature leaving the fuel cell stack is 189 °C, which is within the acceptable range for the fuel cell temperature. The outlet water temperature recovering the heat has a temperature of 92 °C, which is just a little above the goal value of 90 °C. The second recovery circuit is also recovering some heat during this time with the outlet water temperature being 23 °C.

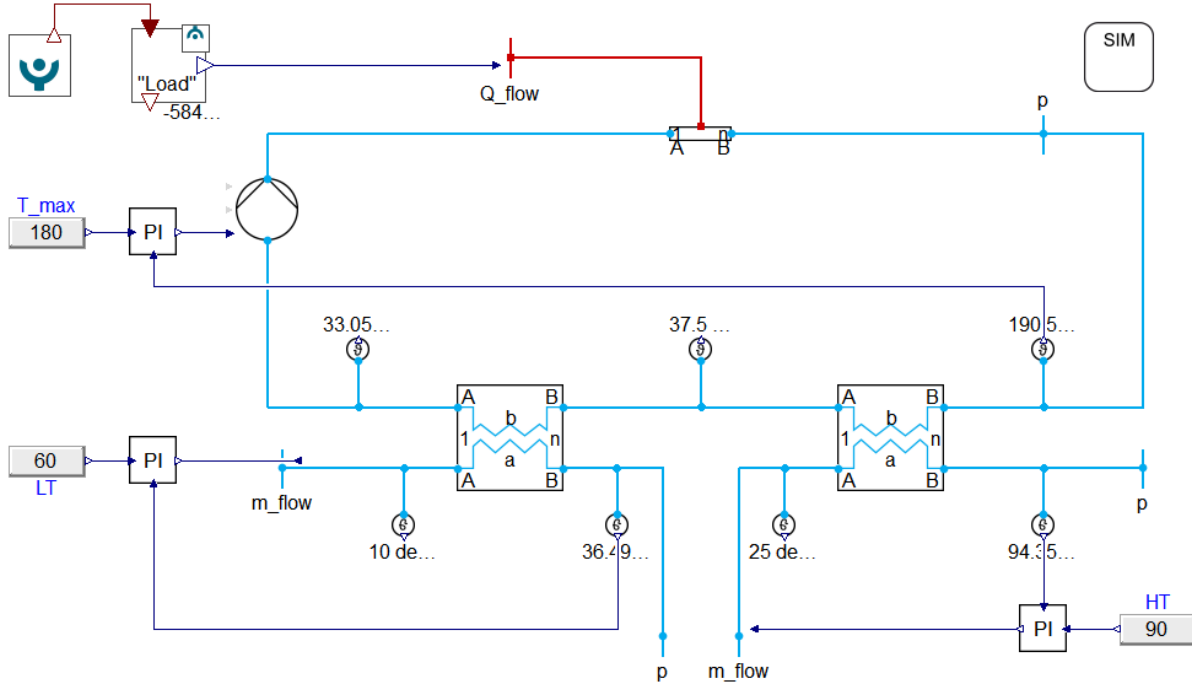


Figure 24: Modelica heat energy recovery model values at maximum heat production.

The heat produced by the fuel cell stack, given in kW, is presented in Figure 25. This is the heat which must be removed by the heat energy recover system.

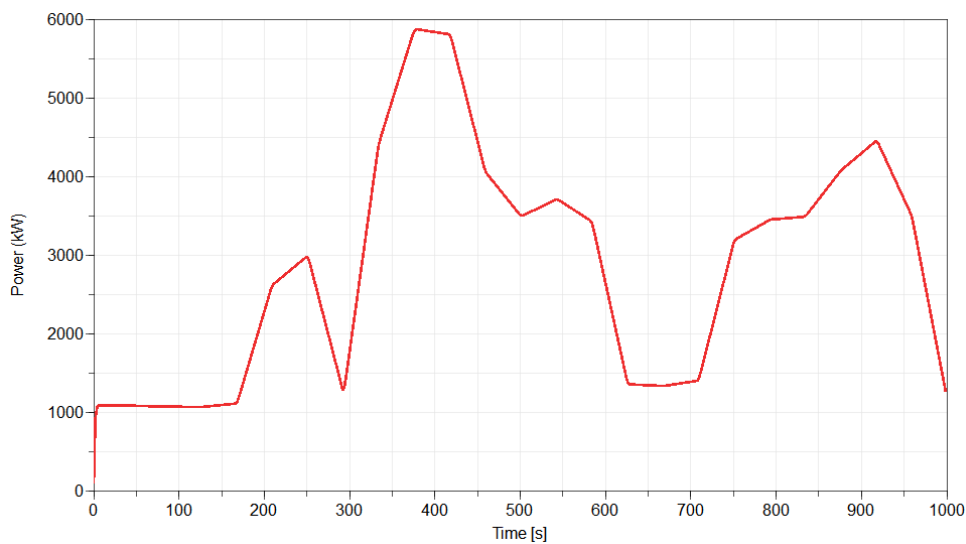


Figure 25: The fuel cell stack's heat production.

The temperature in three different places in the model are presented below. Figure 26 shows the coolant temperature when it leaves the fuel cell stack. The set point temperature is 180 °C, and the actual temperature is in the range from 166 °C to 196 °C. It does not exceed the maximum temperature of 200 °C. It does exceed the working fluid boiling point of 192 °C. The HT recovery circuit has the outlet water temperature presented in Figure 27. The set point is 90 °C and the PI controller is adjusted so the temperature does not exceed 100 °C to keep the water liquid. The range is then between 83 °C and 97 °C. The final temperature presented is for the outlet water in the LT heat energy recover circuit, plotted in Figure 28. It's set point is 60 °C, but the value ranges between 26 and 40 °C when excluding the initial undershooting of the PI controller.

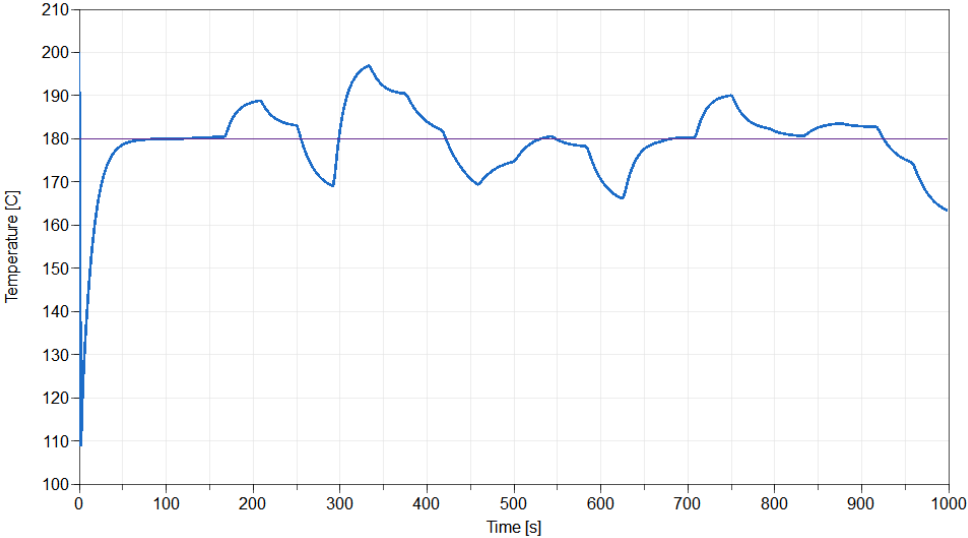


Figure 26: Simulated temperature for the fuel cell stack outlet flow.

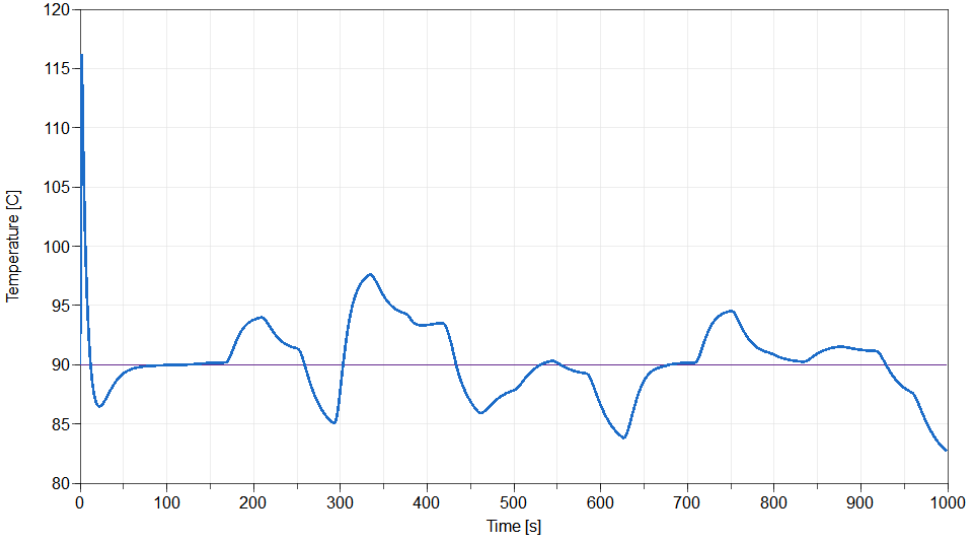


Figure 27: Simulated temperature for the HT recovery stream water outlet.

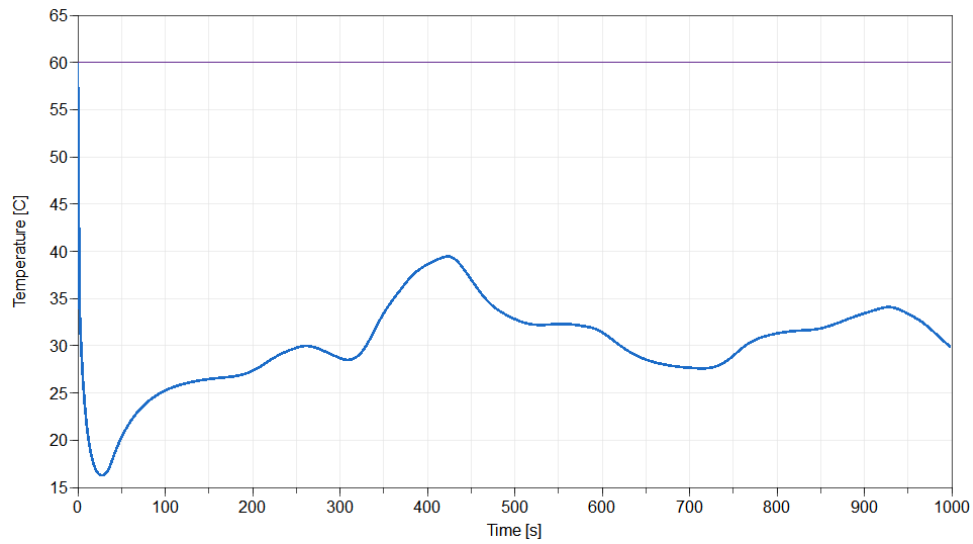


Figure 28: Simulated temperature for the LT recovery stream water outlet.

The mass flow rates of the heat energy recovery model are presented below. The result for the cooling circuit flowing through the fuel cell stack is presented in Figure 29, the HT recovery stream in Figure 30, and the LT recovery stream in Figure 31.

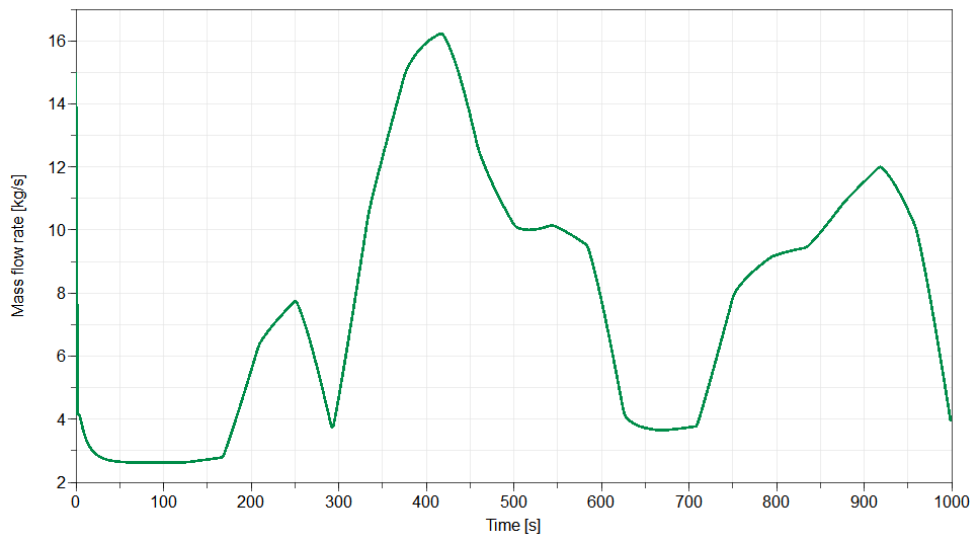


Figure 29: Simulated mass flow rate for the cooling circuit.

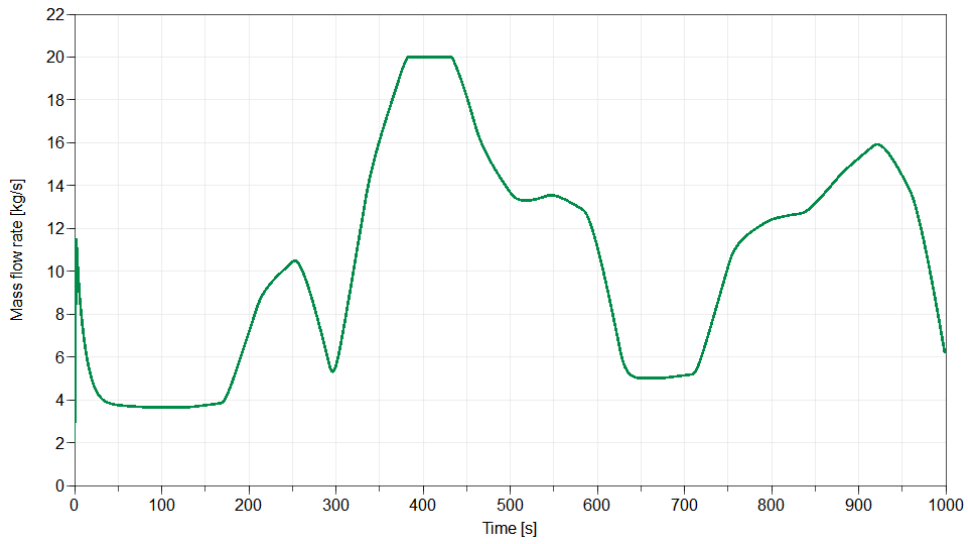


Figure 30: Simulated mass flow rate for the HT recovery stream.

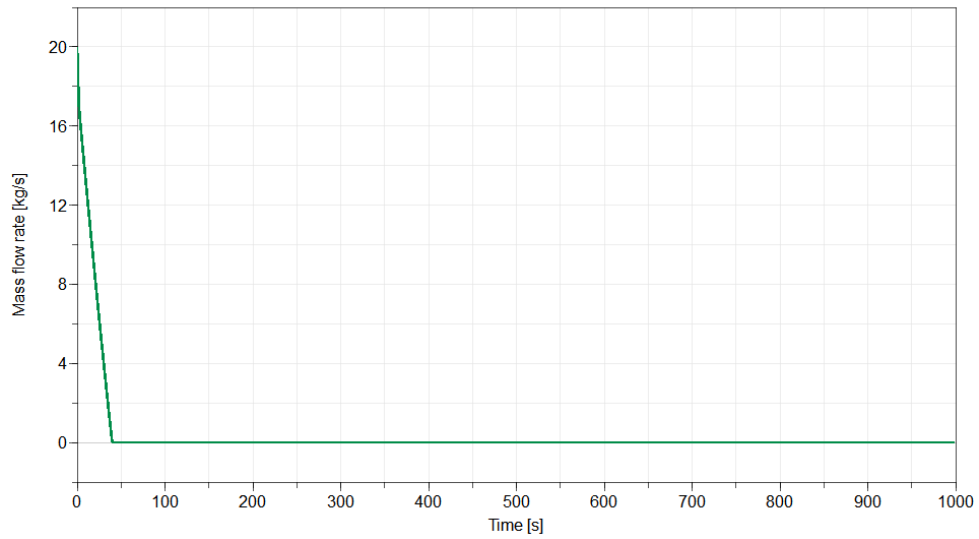


Figure 31: Simulated mass flow rate for the LT recovery stream.

The enthalpy for the HT outlet stream is presented in Figure 32.

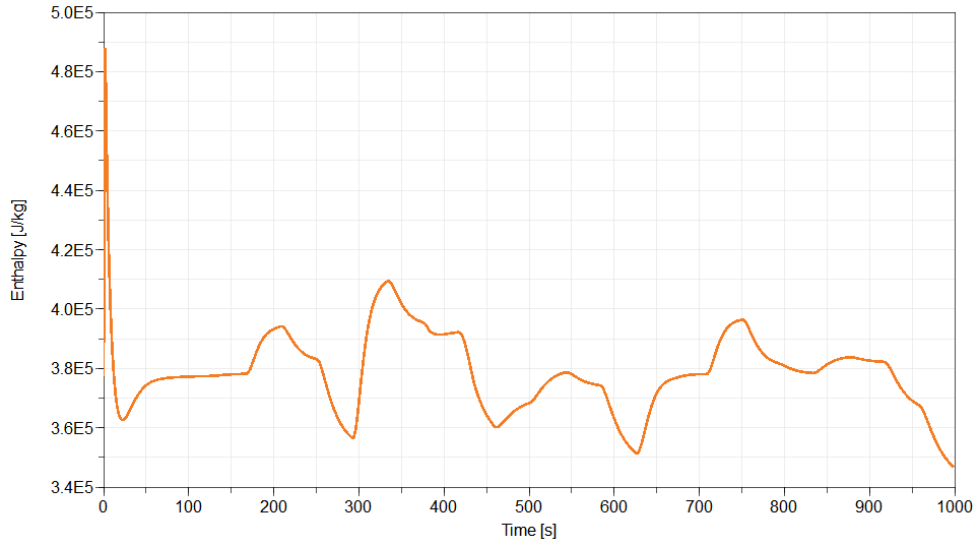


Figure 32: Enthalpy of the outlet stream.

4.6.3 Cold Energy Recovery Model

The results from the cold recovery model from Figure 8 are presented in this section. The hydrogen fuel flow is calculated as described in Section 3.1.3. The profile is presented in Table 16 which shows the hydrogen mass flow rate for each time step. The mass flow rate of the hydrogen through the system is plotted in Figure 33.

Table 16: The hydrogen fuel mass flow rate profile applied to the cold energy recovery model.

Time [s]	MFR [kg/s]
0	0.022
42	0.021
83	0.021
125	0.021
167	0.022
208	0.051
250	0.059
292	0.024
333	0.087
375	0.115
417	0.114
458	0.080
500	0.068
542	0.073
583	0.067
625	0.027
667	0.026
708	0.028
750	0.063
792	0.068
833	0.068
875	0.080
917	0.087
958	0.069
1000	0.022

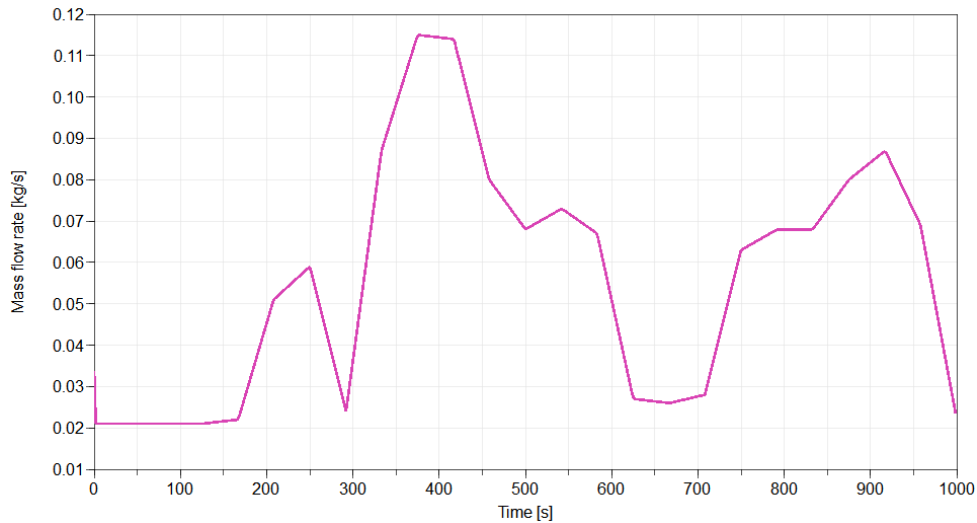


Figure 33: Plot of the hydrogen fuel mass flow rate during simulation.

When running the model, the resulting values at 375 seconds, which is when the fuel flow rate is the highest, are displayed in Figure 34. At this fuel flow rate, the hydrogen is heated to $-102\text{ }^{\circ}\text{C}$ and the outgoing recovery stream temperature is $-90.1\text{ }^{\circ}\text{C}$.

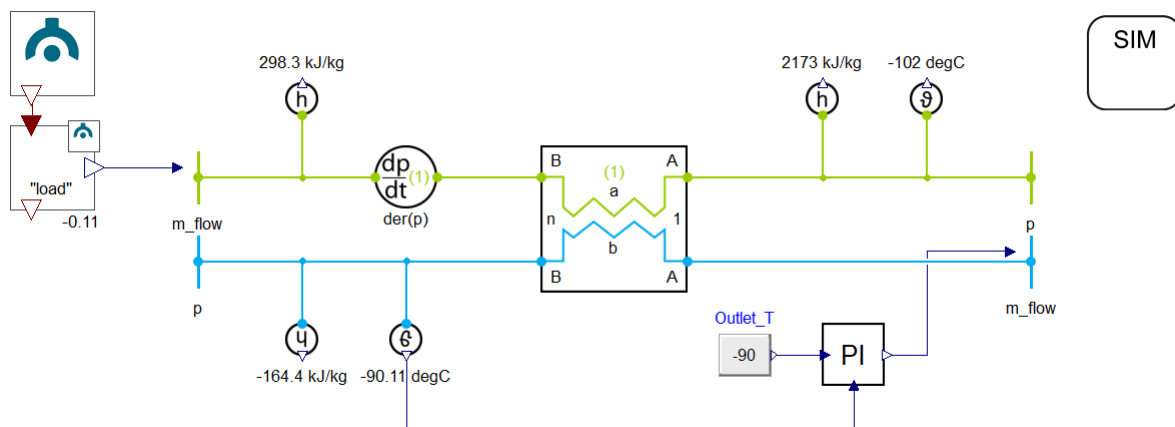


Figure 34: Modelica cold energy recovery model values at maximum hydrogen fuel mass flow rate.

A plot of the hydrogen outlet temperature is presented in Figure 35 and is in the range of approximately -20 to $-110\text{ }^{\circ}\text{C}$. The temperature of the outlet recovery stream, with the set point of $-90\text{ }^{\circ}\text{C}$, is plotted in Figure 36, and stays very close to $-90\text{ }^{\circ}\text{C}$ during the simulation, disregarding the initial start up overshooting.

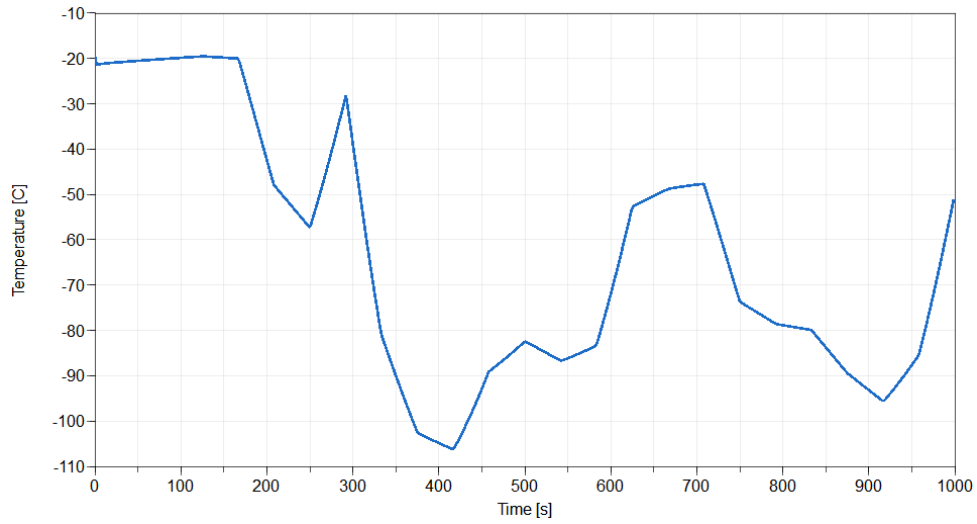


Figure 35: Simulated temperature for outlet hydrogen stream.

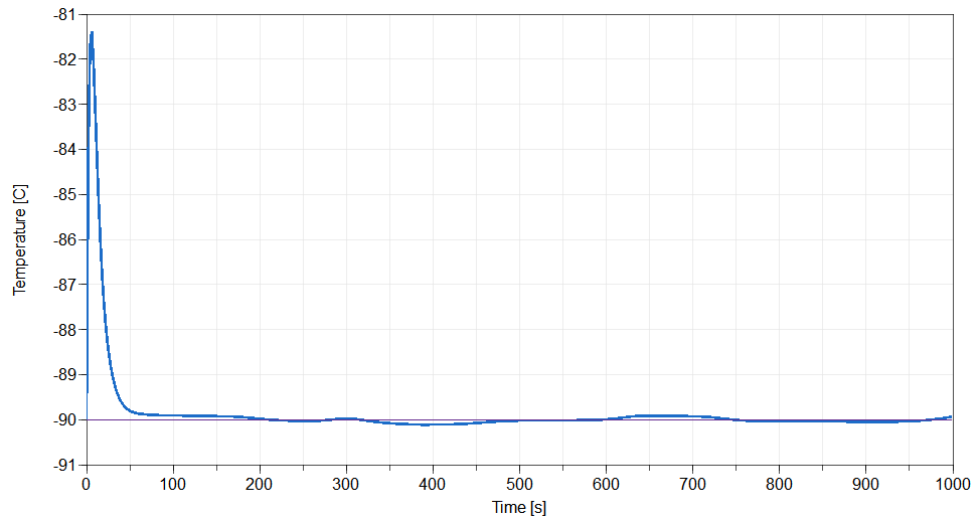


Figure 36: Simulated temperature for the outlet recovery stream.

The mass flow rate of the cold energy recovery stream is plotted in Figure 37. It stays in the range between 0.45 and 0.64 kg per second. The enthalpy of the recovery stream outlet is relatively stable around -160 kJ per kg.

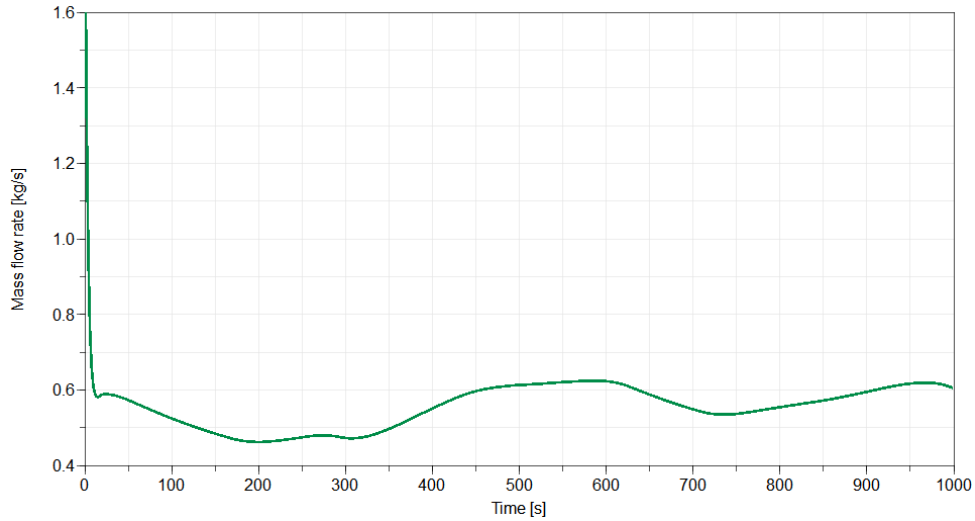


Figure 37: Simulated mass flow rate for the cold energy recovery stream.

The second cold energy recovery model is presented in Figure 8. It includes the reference cooling demand, which load profile is presented in Table 17. It is also based on a time interval of 1000 seconds, as explained in Section 3.2.2. The heat flow into the recovery loop is plotted in Figure 38. The working medium used in the cold recovery circuit is water.

Table 17: The cooling demand load profile applied to the cold energy recovery model.

Time [s]	Cooling demand [kW]
0	1047
42	883
83	933
125	883
167	851
208	982
250	1194
292	1374
333	1227
375	1112
417	1145
458	1129
500	1227
542	1014
583	916
625	998
667	982
708	1047
750	1194
792	1211
833	1112
875	1031
917	982
958	1096
1000	1047

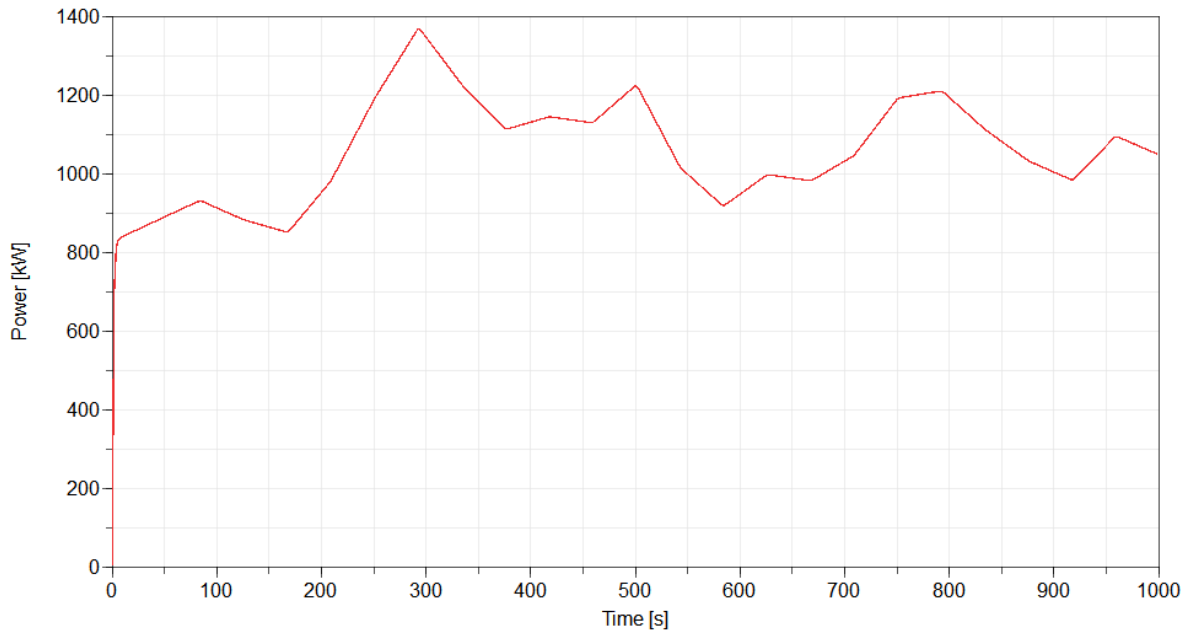


Figure 38: Plot of the cooling demand during simulation.

The hydrogen outlet temperature and the temperatures in the recovery circuit all increase due to accumulation of heat in the cold recovery circuit. Figure 39 is the plots of the hydrogen outlet temperature, the temperature of the cold recovery circuit entering the heat exchanger (Cold recovery 1) and leaving the heat exchanger (Cold recovery 2).

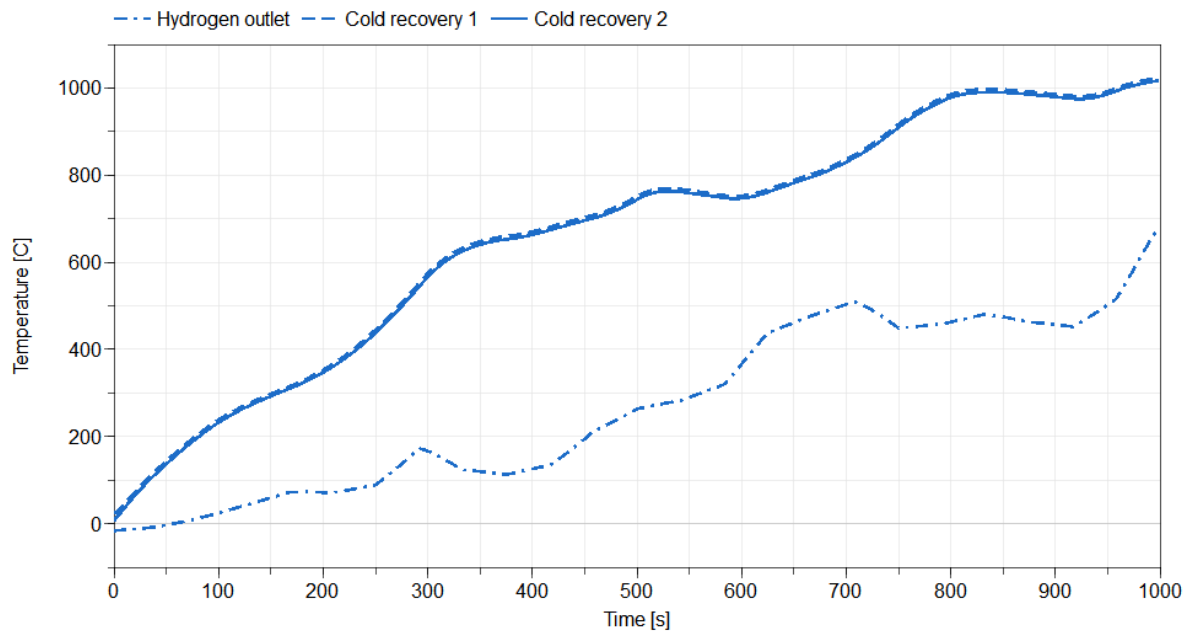


Figure 39: Plot of the temperatures in the second cold energy recovery circuit.

The mass flow rate of the recovery circuit increases exponentially until it reaches the set maximum value.

5 Discussion

As per the research question of this thesis, the main goal of this section is to answer, based on the results, how a hybrid hydrogen fuel cell and battery system should be developed for a cruise ship, while also evaluating the use of TER and TES on its capacity and performance. The cruise ship which this system is applied to is a medium size cruise ship operating in northern climates, based on a real-life ship providing its energy demand profiles. The results are evaluated thoroughly here, and lines are drawn to the literature study.

5.1 System Design

The proposed energy system design for a cruise ship was developed with the goal of being environmentally friendly, innovative, dynamic, and affordable. The main energy source is the fuel cell, which based on the literature study is proposed to be a high temperature PEM fuel cell, as this provides the most efficient production, smooth operation, and compactness needed for maritime applications. It must also be supplied with a battery system to ensure dynamic and reliable energy provision, in addition to drastically reducing the installed power necessary due to peak shaving. This combination should cover electric energy demand on the cruise ship, comprised of propulsion, auxiliary electricity, and any thermal energy top loads.

The thermal energy demands, which make up about half of the total energy demand on a cruise ship travelling a cold climate, should be met primarily with TER with supplementation of top load solutions for peaks in demand. For the hot water demand, which also comprises of space heating through water, this means heat energy recovery from the fuel cell and battery system and electric boilers for top loads, supplied by the fuel cell and battery system. For the space cooling demand, most of it can be covered through "cold energy" recovery from the liquid hydrogen regasification process, which is supplied to a CO₂ refrigeration heat pump unit. This unit works well for maritime applications due to zero emissions, lower electricity demand, and higher safety than alternative heat pumps. The cooling unit is supplied with electricity from the fuel cell and battery system. Having the entire energy system based on electricity, as opposed to part electricity and part LNG or oil fuels, allows for more dynamic energy production management and better optimisation.

The thermal management of the fuel cell and battery is necessary to keep the system from overheating, which would lead to lower electrical efficiency, shorter component lifetime, and safety issues. Based on the literature study, a liquid based thermal management system with dedicated cooling channels through the fuel cell stack is the best solution when considering efficiency and costs. For medium temperature ranges, water is a good coolant choice, but for the high temperature fuel cell used for this project, other options must be considered which have boiling temperatures exceeding the FC stack operating temperature. Several coolants were evaluated, both based on theory and on simulations. The most important factors to consider are the boiling point, flash point, and heat capacity and conductivity. The working fluids will be discussed further in Section 5.5.

The hydrogen fuel storage and management were also evaluated. There are several ways to store fuel for hydrogen fuel cells, but the one considered for this project is as pure liquid hydrogen. Based on the literature study, this is appropriate for maritime applications of this size and range. This is the most compact solution, which would be highly beneficial for a cruise ship as it would allow for more passenger cabins and thus higher income during operation. LH₂ is stored in a tank under 1 atmosphere pressure, which is well isolated to maintain the cryogenic temperature of the fuel and avoid boil-off losses. The storage capacity might pose an issue. Although the gravimetric energy density of LH₂ is high, the volume needed to store such large quantities of hydrogen to fuel the system poses a challenge. This is especially challenging for cruise ships travelling for several days before having to the opportunity to refuel at a port.

Before entering the fuel cell, the liquid hydrogen must be converted back into hydrogen gas of room temperature for optimal fuel cell operation. This regasification process leads to very low temperatures of the heating medium, which traditionally has been released directly to the external environment. By utilising the medium on board the ship, energy savings can be achieved.

The electricity consumption for the reference ship space cooling can be greatly reduced by switching out the compression chiller system with a CO₂ heat pump refrigeration solution. The COP would be several times higher, leading to significant reductions in electricity consumption with the same cooling power delivered. Although the annual space cooling demand is relatively low compared to the other energy demands, it could still contribute to cost savings. In addition, for the reference case only space cooling is covered by the chiller system, but other energy demands can be covered as well. These include provision cooling and freezing, dehumidification, and some other cooling demands. Allocating this to the cooling demand would reduce some of the auxiliary electricity demand and since the energy efficiency would be higher with a CO₂ system, the overall energy demand would be reduced.

5.2 Reference Case Evaluation

There are certain sources of error regarding the reference case which must be considered when evaluating the results. Firstly, the reference ship, Birka, runs on heavy fuel oil, meaning that some of the heating demand relates to heating this fuel. This energy demand is not directly applicable to an fully electric vessel. However, some heating may still be required for the regasification of liquid hydrogen if this is not covered through the cold recovery for the space cooling demand. Especially in winter and spring/fall conditions, where the space cooling is negligible, the hydrogen must be heated by other means. This can be done through air or seawater taken directly from outside, but as the hydrogen gas should hold room temperature before entering the fuel cell, further heating might be necessary. Therefore, the energy demand of the proposed system has been considered similar to the reference case in this project. This can be more thoroughly evaluated in further research.

The energy demand of the cruise ship varies due to changing ambient temperature conditions during the year in Sweden where Birka operates. Data from the reference case was given based on the season, where spring and fall is combined due to similar temperatures. The power needed for propulsion and auxiliary electricity is considered constant during the year, so the change in power based on season is due exclusively to thermal demands. During winter, the heating demand is significant due to low ambient temperatures and thus high space heating demand. This leads to winter conditions having the highest energy and peak power demand. The space heating demand in summer is most likely negligible, but due to domestic hot water demands there is still a heating demand for summer conditions. Combined with the space cooling demand, which is only prominent during summer, this season has the second highest energy and peak power demands. For spring and fall conditions, the heating demand is higher than for summer, but due to the lack of space cooling demand, leaves the spring/fall season with the lowest energy and peak power demand. It is assumed for this thesis, based on the literature study, that winter temperatures last for 182 days, summer last for 62 days, and spring and fall combined lasts for 121 days. This is based on an estimate of Swedish temperatures and can be altered corresponding to the application area.

Overall, the reference case used for this project seems like a good base for calculations. The Birka cruise ship reference case is a good representation for medium size cruise ships operating in Nordic climates. With the three different scenarios representing different seasons included, a wider range of energy demands has been evaluated as well, leading to results with a wider application range. For example, summer conditions can be applied as the average demand for cruise ships operating in warmer climates. The hotel energy loads for Birka compared to the total energy load is approximately 40% for spring/fall conditions, which corresponds well with the literature study.

5.3 Thermal Recovery and Storage

The electrical efficiency of the fuel cell is estimated at 50%, meaning that about half the hydrogen fuel energy supplied is converted to electrical energy. Due to fuel and heat losses in the fuel cell, approximately 36% of the fuel energy is converted to recoverable heat. Thus, when fully exploited, the recovered heat energy from the fuel cell increases the fuel cell efficiency from 50% to 86%. In reality the actual heat energy recovered will vary based on the temperature levels, thermal energy demand, and various losses from transfer and storage. Implementing TER in the system will lead to a lower design capacity of the fuel cell, reduced fuel consumption, and reduced fuel storage capacity. TES does not affect the design capacity but does reduce the fuel consumption and storage capacity.

The maximum power demand peak of the cruise ship determines the needed fuel cell and battery capacity. This peak occurs at 9 am during winter conditions. At this time, the thermal percentage of the load is relatively low, meaning that the entire heating demand can be covered through heat energy recovery. The power peak is reduced by 32.7% with TER, meaning that the fuel cell installed power also can be reduced with the same percentage. This will reduce the fuel cell stack size and thus also significantly reduces the

investment costs of the fuel cell system. TES does not reduce the peak further since the heat demand at this hour is already fully covered.

The fuel storage capacity is determined based on the day with the highest fuel consumption, which occurs during winter. The amount of fuel needed in wintertime is reduced by 30.8% with TER, meaning that the storage capacity can be reduced accordingly. When including TES, the storage capacity is reduced by another 3.1% points. The storage reduction would reduce both the investment and operational costs significantly. With the volume reduction, less storage space is needed, and more space is available for cabins for more passengers. The weight reduction leads to less fuel consumption, and thus lower operational costs. As TER shows such a large reduction, it seems highly beneficial for the cruise ship energy system. TES implementation might need further analysis of cost savings and emission reduction.

The annual fuel consumption is reduced when including thermal recovery, both hot and cold, and when including thermal storage. The annual fuel consumption is reduced by 30.1% with TER and by another 3.7 % points when including TES. This corresponds to 992 and 1117 tonnes of LH₂ saved every year. Due to the relatively high price of LH₂, this corresponds to significant annual savings.

The cold energy recovery and storage makes up a relatively small percentage of the savings. This is because the cooling demand makes up a smaller part of the power load during summer and is negligible in the much longer winter and spring/fall scenarios. If including a CO₂ cooling system, the cooling demand would be even less significant.

5.4 System Capacity and Battery Influence

The design system capacity is determined by the maximum peak power occurring during any season, as the system must be able to cover the highest power demand occurring during the year. For the reference case, this peak happens during winter conditions at 9 am. Without any TER or TES, the capacity must be at least 12.12 MW. This is large compared to current PEM fuel cell installations, but not impossible based on projects planned for implementation in the near future. However, when introducing TER, the capacity is reduced to 8.16 MW. This number is not affected by the inclusion of TES.

The battery used in combination with the fuel cell should be designed to cover about 20% of the total installed power of the energy system. This would compensate for the poor dynamic response of fuel cells compared to oil fuelled motors. It would also lead to peak shaving, thus reducing the necessary installed power of the system. The reason for not covering a larger part of the load with a battery is the additional size required due to lower energy density. This means that there is a trade-off point between fuel cell and battery coverage which must be calculated to determine the exact division of installed power. For now, 20% is assumed to be a good starting point.

The battery is charged and discharged based on the electricity production curve of the HFC when TER and TES are included. It is fully discharged during peak hours to reduce the

necessary fuel cell installed power. It is charged again by the fuel cell during power valleys to reduce the dynamic fluctuations of production by the HFC. The charging and discharging are performed several times to smooth out the production curve as much as possible, all while avoiding overcharging the battery capacity. The final electricity production is less volatile, although a larger battery is necessary to smooth it out properly.

The resulting reduction in necessary installed power for the fuel cell is 10.6%. This means that the final battery capacity is 1.63 MW and the final fuel cell capacity is 7.30 MW, with the combined capacity of 8.93 MW. These values are large compared to existing systems in the transportation sector. However, as explored in the literature study, the feasible capacity of fuel cells is steadily increasing. In addition, the system size can be reduced with higher electric energy efficiency of the fuel cell or a larger battery coverage percentage. Therefore, there is a possibility for this type of capacity to be realistic in the future.

5.5 Simulation Evaluation

The models created in Modelica were developed from scratch and are therefore fairly basic with much potential for further expansions and optimising. There are areas that work well, while others need improvement to yield useful results when simulated. The heat energy recovery model works well based on resulting temperatures, while the different cold recovery models show some issues with the heat transfer and resulting temperatures. They will all be discussed in this section with more suggestions for further improvements and expansions in Section 7.

5.5.1 Heat Transfer Fluid Choice

The heat transfer fluid used for all simulations was Therminol D-12, based on the initial coolant testing. When comparing the three Therminol fluids, D-12 resulted in the lowest cooling circuit mass flow rate, with 59 and 66 resulting in higher flow rates, in that order. Although the thermal conductivity is the lowest for D-12, it still lead to a more efficient system. This might be due to its higher specific heat capacity. Its recommended bulk use temperature is also closer to the maximum system operating temperature of 200 °C. Another benefit of this medium is that its minimum use temperate of -94 °C is much lower than the two others, which makes it useful also for cold energy recovery. On the other side, its recommended bulk use temperature and boiling points are much lower than for the two others. Its boiling point of 192 °C is close to the fuel cell operating temperature of around 180 °C, which might cause issues with pumping the fluid. Another downside of D-12 is the flash point temperature of 62 °C, which is very close to the safety temperature of minimum 60 °C for maritime applications. The other two Therminol heat transfer fluids have much higher flash point temperatures. This means that the other two fluids, and especially Therminol 59, should also be considered when selecting a fitting working medium for the systems.

There are other coolants available in Modelica which also can be used for testing, as long as their working temperature ranges are within the limits of the system. From the simulation comparing water and propylene glycol mixed with water, the PG/W mixture

yielded better results than pure water, despite water having higher thermal conductivity. This was because the maximum temperature of the coolant could be increased from 99 to 105 °C. In other words, a small change in temperature had a bigger impact than a large change in thermal conductivity. Thus, only coolants with boiling points above 180 °C should be considered, even if other coolants have better thermal conductivity. As long as the coolant meets the temperature demand, the optimal option would be the one with the best thermal conductivity, lowest cost, good safety range, and lowest environmental effect, both in terms of GHG emissions and negative human health effects.

5.5.2 Heat Energy Recovery Model Evaluation

The heat energy recover model works as intended. The heat load profile applied to the heat energy recovery is read properly by the system. The model keeps the operating temperature of the fuel cell at its optimum of approximately 180 °C under constant heat load, which is the set point temperature chosen. When varying the heat load according to the reference case profile, it stays in the range of about 166 to 196 °C. This is within an acceptable range for the fuel cell operating temperature. However, it does at times exceed the working fluid boiling point of 192 °C, which would cause issues with the medium circulation and properties. This can be solved by choosing a different heat transfer fluid, slightly reducing the set point temperature at the cost of a slightly less efficient fuel cell or improving the PI controller to avoid oscillations in the temperature.

The high temperature hot water production also works well in the model. The exiting water stream keeps a temperature in the range of 83 to 97 °C, which is relatively close to the set point temperature of 90 °C. It is also important that it does not exceed 100 °C to avoid boiling of the water, which was achieved by slightly adjusting the PI controller, reducing temperature oscillations.

When it comes to the model which includes a low temperature hot water stream, it should be further developed. The HT stream still works well, producing 90 °C temperature water. However, there is no regulation on how much HT water is needed, so almost all heat energy recover happens in this circuit, while very little is left for the LT stream. The LT stream can be regulated either with the goal of reaching 60 °C or with the goal of reducing the temperature of the stack cooling circuit down to a determined value. The former option results in the highest temperatures of the outlet stream, but still only reaches 40 °C by reaching the minimum mass flow rate value of almost zero. There is still some available heat in the cooling circuit as well which is not transferred due to the low mass flow rate. When adjusting the flow such that the cold side of the stack cooling circuit holds 10 °C, the mass flow rate is very high, and the temperatures of the LT hot water is therefore also lower. The goal should be to stay close to the optimal value of 60 °C, which is the set point in the model. This can be achieved by adding regulation on the mass flow rate of the HT flow based on the HT water demand. Data on the LT and HT hot water demand division was not available from the reference case but can be estimated based on other cases or similar systems for future work.

The mass flow rates calculated in the simulations are relatively high due to the high

PEMFC heat production rate. For the model, a single recovery circuit was made, and only one or two recovery streams were made, for simplicity. In reality, the pumping capacity available for the chosen pump will decide if and how many parallel streams are necessary to achieve the required mass flow rate.

5.5.3 Cold Energy Recovery Model Evaluation

The first cold energy recovery model, which is the simplest one, works as intended in regard to temperatures. The hydrogen flow profile from the reference case loads properly. The recovery flow is cooled by the hydrogen flow through the heat exchanger and keeps the set point outlet temperature by regulating its mass flow rate. The set point is chosen as $-90\text{ }^{\circ}\text{C}$, since this is the minimum use temperature of the heat transfer fluid used but can easily be changed. With higher hydrogen mass flow rate comes higher recovery mass flow rate and lower outgoing hydrogen flow temperature. This means that the system handles low hydrogen flow better, where more heat can be transferred from the recovery stream to the hydrogen stream. The goal should be to reach room temperature of the outgoing hydrogen so it can be supplied to the fuel cell. This is achieved by decreasing the hydrogen fuel flow. When having the hydrogen flow following the reference case profile, it must be achieved some other way, for example by changing the heat transfer fluid, increasing the heat exchanger capacity, or using several recovery streams with heat exchangers.

With the current simple model, the highest hydrogen mass flow rate required of $0.115\text{ kg per second}$ leads to an outlet temperature of $-138\text{ }^{\circ}\text{C}$. This is significantly higher than the initial temperature of $-253\text{ }^{\circ}\text{C}$, but also far from room temperature. The hydrogen flow must be $0.003\text{ kg per second}$ to provide an outlet temperature of $20\text{ }^{\circ}\text{C}$. This is much lower than the streams in the reference case mass flow profile, so the model requires changes like several recovery streams or larger capacity heat exchangers. Several heat exchangers are also beneficial for a more easily regulated system where the stream can bypass one or more exchangers during lower hydrogen flow rate.

The second cold energy recovery model, which uses a water circuit to transfer cold energy from the hydrogen flow to the cold sink which represents the space cooling device, does work based on the way it is modelled. The heat flow into the water circuit, which represents the cold sink, loads properly. It is also transferred to the hydrogen stream, heating the hydrogen as intended. However, the issue with the model is that the heat stream is very large, meaning that it accumulates both in the water circuit and in the hydrogen stream, leading to extremely high temperatures by the end of the simulation time. This means that the hydrogen is not able to absorb all the heat applied to the system and further cooling is needed.

The other cold energy recovery models, which are more complex, have more issues with simulation, due to the low temperatures used. The ones added in the Appendix were intended as exploration of different options for cold recovery in combination with a CO_2 stream and in combination with heat energy recovery from the fuel cell stack. These are suggestions that can be further developed, but which do not provide especially useful results for this project and will therefore not be discussed further. Ideally, the cold recovery

model should be a combination of hydrogen regasification and a CO₂ refrigeration heat pump model, with hydrogen flow rate and space cooling demand implemented. This would provide a fuller evaluation of the feasibility and possible energy savings of the system.

6 Conclusion

As an answer to the research question, the energy system in this thesis is developed for a medium sized cruise ship operating in northern climates. It consists of a PEM hydrogen fuel cell with approximately 7.3 MW of installed electrical power and a battery system with the maximum charging capacity of about 1.6 MW. Their combined capacity is 8.9 MW. The PEMFC provides electricity for propulsion of the ship and auxiliary electricity needs on board, where the battery covers top loads. The hydrogen supplied to the FC is stored as a cryogenic liquid in tanks on board. The fuel cell solution would lead to less emissions of CO₂, NO_x, and SO₂, which is necessary for cruise ships to enter Norwegian fjords in the future, as well as many international ports. It also provides overarching energy management and quieter operation.

The hot water demand, which encompasses space heating demand, is covered through heat energy recovery from the HFC, where some of this energy is stored in hot water tanks. During winter, when the hot thermal energy demand is higher than what can be recovered, the top load is covered by electric boilers supplied by the HFC and battery. The space cooling demand is covered by cold thermal energy recovered from the regasification process of the LH₂, which is supplied to a CO₂ refrigeration heat pump unit driven by electricity from the HFC and battery. The TER implementation led to over 30% reduction of the installed power needed for the HFC and battery, fuel storage capacity needed on board, and annual fuel consumption. Implementation of TES in addition to TER led to a more modest reduction of around 3 additional percentage points.

The Modelica simulations developed for the thesis mostly run as expected with regards to heat transfer and temperature changes, which makes them seem like a solid initial setup. It forms a good basis for further expansion and improvements for a closer approximation to the real-life system. The mass flow rates are high due to the high installed power of the system, but this can be reduced by adding several parallel thermal recovery systems. The temperatures are realistic and stable with a full heat energy recovery from the fuel stack cooling loop. The cold energy recovery models require further work in terms of dimensioning. The models also provide a good tool for comparing different coolants in terms of efficiency, although other coolant properties and options not available in the TIL library also should be evaluated.

The initial installed power needed for the PEMFC is high compared to existing solutions but should become feasible in the near future. TER leads to significant cost savings in terms of less investment of equipment, more space for passenger cabins, and lower fuel consumption. Due to the necessity of a thermal management system for the HFC regardless of recovery, the additional costs of TER would be relatively small. TES also contributes to these savings, but less significantly so, and it also requires storage space and additional management. Therefore, TER is highly recommended for HFC driven cruise ships, while TES probably requires further cost-benefit analyses.

7 Further Work

The energy system can be further developed with more technical details of the setup of the HFC, battery, thermal energy recovery systems, and CO₂ cooling unit. The recovered energy uses should also be further investigated, where proper numbers on the HT and LT hot water demands are used to determine how much heat energy can be feasibly recovered.

The models used for simulation should be expanded and optimised. One goal should be to reduce the mass flow rates of the liquids. This can be done by testing different coolants and by changing the temperature restrictions accordingly. The heat exchange can also be performed in several stages, so the temperature of the outgoing flow is well fitted for its purpose, whether this is domestic hot water production, thermal heat storage, or seawater desalinisation. One should also aim for achieving feasible, stable temperatures not only for the heat energy recovery, but for the cold energy recovery models as well.

The models can also be expanded to include more components for a more realistic simulation. First, the CO₂ refrigeration system in the cruise ship can be connected to the cold recovery to explore this potential properly. The thermal storage system should also be incorporated in the model. The battery influence could also be evaluated and incorporated in Modelica, if possible.

Finally, perspectives like the economic and environmental impacts should be evaluated in future projects. A profitability analysis would give vital insight into whether a HFC and battery solution could be feasible for maritime applications. It should also be performed when regarding TER and TES, especially the latter as it is more uncertain if this is profitable. A greenhouse gas emission analysis would also be very useful since much of the motivation behind the project is to reduce the negative environmental impact from the cruise ship sector.

References

- [1] Francesco Baldi, Fredrik Ahlgren, Francesco Melino, Cecilia Gabriellii, and Karin Andersson. Optimal load allocation of complex ship power plants. *Energy Conversion and Management*, 124:344–356, 2016. doi: 10.1016/j.enconman.2016.07.009.
- [2] J. Han, J.-F. Charpentier, and T. Tang. An energy management system of a fuel cell/battery hybrid boat. *Energies*, 7(5):2799–2820, May 2014. doi: 10.3390/en7052799.
- [3] IMO. Initial imo ghg strategy, 2021. URL <https://www.imo.org/en/MediaCentre/HotTopics/Pages/Reducing-greenhouse-gas-emissions-from-ships.aspx>. Accessed: 22.11.21.
- [4] Nor-Shipping. Norway’s new emission free cruise ship concept, 2021. URL <https://www.nor-shipping.com/norways-new-emission-free-cruise-ship-concept>. Accessed: 22.11.21.
- [5] Port of Oslo. Zero-emission port, 2021. URL <https://www.oslohavn.no/en/menu/klima-og-miljo-i-oslo-by-og-havn/zero-emissions-port/>. Accessed: 22.11.21.
- [6] Marit Nilsen. Zero emissions in the world heritage fjords by 2026. Norwegian Maritime Authority (Sjøfartsdirektoratet), April 2022. URL <https://www.sdir.no/en/news/news-from-the-nma/zero-emissions-in-the-world-heritage-fjords-by-2026/>.
- [7] SINTEF. Cruize - utvikling av innovative og integrerte kjøle- og oppvarmingskonsepter om bord i cruiseskip, November 2020. URL <https://www.sintef.no/prosjekter/2020/cruize/>. Accessed: 23.11.21.
- [8] B. Veldhuizen, R. Hekkenberg, and L. Codiglia. Fuel cell systems applied in expedition cruise ships - a comparative impact analysis. *HIPER*, 2020. URL https://www.researchgate.net/publication/344606626_Fuel_Cell_Systems_Applied_in_Expedition_Cruise_Ships_-_A_Comparative_Impact_Analysis.
- [9] M.Z. Saeed, A. Hafner, C.H. Gabriellii, I. Tolstorebrov, and K.N. Widell. Co2 refrigeration system design and optimization for lng driven cruise ships. *CRISTin - NTNU*, 2021. doi: 10.18462/iir.nh3-co2.2021.0015.
- [10] M.A. Ancona, F. Baldi, M. Bianchi, L. Branchini, F. Melino, A. Peretto, and J. Rosati. Efficiency improvement on a cruise ship: Load allocation optimization. *Energy Conversion and Management*, 164:42–58, 2018. doi: 10.1016/j.enconman.2018.02.080.
- [11] Convert eer to cop and cop to eer (calculator). LearnMetrics. URL <https://learnmetrics.com/convert-eer-to-cop/>. Accessed: 27.05.2022.
- [12] Rene Langer. Convert eer to cop and cop to eer (calculator + table). PickHVAC, April 2022. URL <https://www.pickhvac.com/calculator/eer-to-cop/>.
- [13] Tzong-Shing Lee. Second-law analysis to improve the energy efficiency of screw liquid chillers. *Entropy*, 12, March 2010. doi: 10.3390/e12030375.

- [14] F.W. Yu, K.T. Chan, R.K.Y. Sit, and J. Yang. Review of standards for energy performance of chiller systems serving commercial buildings. *Energy Procedia*, 61: 2778–2782, 2014. doi: 10.1016/j.egypro.2014.12.308. International Conference on Applied Energy, ICAE2014.
- [15] H.Q. Nguyen and B. Shabani. Proton exchange membrane fuel cells heat recovery opportunities for combined heating/cooling and power applications. *Energy Conversion and Management*, 204(112328), January 2020. doi: 10.1016/j.enconman.2019.112328.
- [16] U.S. Department of Energy. Fuel cells. *Fuel Cell Technologies Office*, November 2015.
- [17] H. Xing, C.S., S. Spence, and H. Chen. Fuel cell power systems for maritime applications: Progress and perspectives. *Sustainability*, 13(1213), 2021. doi: 10.3390/su13031213.
- [18] R.E. Rosli, A.B. Sulong, W.R. W. Daud, M.A. Zulkifley, T. Husaini, M.I. Rosli, E.H. Majlan, and M.A. Haque. A review of high-temperature proton exchange membrane fuel cell (ht-pemfc) system. *International Journal of Hydrogen Energy*, 42(14):9293–9314, April 2017. doi: 10.1016/j.ijhydene.2016.06.211.
- [19] C. Zhang, W. Zhou, M. Mousavi Ehteshami, Y. Wang, and S.H. Chan. Determination of the optimal operating temperature range for high temperature pem fuel cell considering its performance, co tolerance and degradation. *Energy Conversion and Management*, 105:433–441, November 2015. doi: 10.1016/j.enconman.2015.08.011.
- [20] Wikipedia. Proton-exchange membrane fuel cell, 2021. URL https://en.wikipedia.org/wiki/Proton-exchange_membrane_fuel_cell. Accessed: 24.11.21.
- [21] N. Shakeri, M. Zadeh, and J.B. Nielsen. Hydrogen fuel cells for ship electric propulsion. *IEEE Electrification Magazine*, June 2020. doi: 10.1109/MELE.2020.2985484.
- [22] B. Radowitz. World’s first liquid hydrogen fuel cell cruise ship planned for norway’s fjords. Recharge, 3 February 2020. URL <https://www.rechargenews.com/transition/world-s-first-liquid-hydrogen-fuel-cell-cruise-ship-planned-for-norway-s-fjords/2-1-749070>. Last updated: 05.02.2020.
- [23] Office of Energy Efficiency & Renewable Energy. Hydrogen storage, 2021. URL <https://www.energy.gov/eere/fuelcells/hydrogen-storage>. Accessed: 10.11.21.
- [24] A. Züttel. Hydrogen storage methods. *Naturwissenschaften*, 91:157–172, March 2004. doi: 10.1007/s00114-004-0516-x.
- [25] Engineering ToolBox. Fuels - higher and lower calorific values, 2003. URL https://www.engineeringtoolbox.com/fuels-higher-calorific-values-d_169.html. Accessed: 03.11.21.
- [26] Demaco. The energy density of hydrogen: a unique property, 2021. URL <https://demaco-cryogenics.com/blog/energy-density-of-hydrogen/>. Accessed: 26.11.21.
- [27] A. Baroutaji, A. Arjunan, M. Ramadan, J. Robinson, A. Alaswad, M.A. Abdelkareem, and A.-G. Olabi. Advancements and prospects of thermal management and waste heat

- recovery of pemfc. *International Journal of Thermofluids*, 9(100064), February 2021. doi: 10.1016/j.ijft.2021.100064.
- [28] U. Soupremanien, S.L. Person, M. Favre-Marinet, and Y. Bultel. Tools for designing the cooling system of a proton exchange membrane fuel cell. *Applied Thermal Engineering*, 40:161–173, 2012. doi: 10.1016/j.applthermaleng.2012.02.008.
- [29] M.R. Islam, B. Shabani, G. Rosengarten, and J. Andrews. The potential of using nanofluids in pem fuel cell cooling systems: A review. *Renewable and Sustainable Energy Reviews*, 48:523–539, 2015. doi: 10.1016/j.rser.2015.04.018.
- [30] A. Arsalis, M.P. Nielsen, and S.K. Kær. Modeling and simulation of a 100 kwe ht-pemfc subsystem integrated with an absorption chiller subsystem. *International Journal of Hydrogen Energy*, 37(18):13484–13490, September 2012. doi: 10.1016/j.ijhydene.2012.06.106.
- [31] Norwegian Maritime Authority. Regulations on ships using fuel with a flashpoint of less than 60°C and other regulatory amendments – implementation of the igf code. *No. 2016/63533-36/avi*, December 2016.
- [32] Therminol. Heat transfer fluids, 2021. URL <https://www.therminol.com/heat-transfer-fluids>. Accessed: 10.12.2021.
- [33] Eastman. Selection guide - high performance fluids for precise temperature control, 2021. URL <https://www.therminol.com/sites/therminol/files/documents/TF8691.pdf>. Accessed: 17.12.2021.
- [34] M.H.S. Bargal, M.A.A. Abdelkareem, Q. Tao, J. Li, J. Shi, and Y. Wang. Liquid cooling techniques in proton exchange membrane fuel cell stacks: A detailed survey. *Alexandria Engineering Journal*, 59(2):635–655, April 2020. doi: 10.1016/j.aej.2020.02.005.
- [35] N. Ghaffour, J. Bundschuh, H. Mahmoudi, and M.F.A. Goosen. Renewable energy-driven desalination technologies: A comprehensive review on challenges and potential applications of integrated systems. *Desalination*, 365:94–114, January 2015. doi: 10.1016/j.desal.2014.10.024.
- [36] M. Yang, S. Hu, F. Yang, L. Xu, Y. Bu, and D. Yuan. On-board liquid hydrogen cold energy utilization system for a heavy-duty fuel cell hybrid truck. *World Electric Vehicle Journal*, 12(136), August 2021. doi: 10.3390/wevj12030136.
- [37] J.O. Khor, F.D. Magro, T. Gundersen, and A. Romagnoli. Recovery of cold energy from lng regasification: applications beyond power cycles. *Energy Conversion and Management*, 174:336–355, October 2018. doi: 10.1016/j.enconman.2018.08.028.
- [38] G. Pasini, A. Baccioli, L. Ferrari, and U. Desideri. Potential energy recovery from lng regasification in lng-fueled ships. *SUPEHR19*, 1, 2019. doi: 10.1051/e3sconf/201911302011.
- [39] C. Powars and T. Derbidge. Liquefaction energy recovery in lng and lh2 fueled vehicles. *SAE International*, August 2000. doi: 10.4271/2000-01-3082.

- [40] Enrico Baldasso, Maria E. Mondejar, Stefano Mazzoni, Alessandro Romagnoli, and Fredrik Haglind. Potential of liquefied natural gas cold energy recovery on board ships. *Journal of Cleaner Production*, 271:122519, 2020. doi: 10.1016/j.jclepro.2020.122519.
- [41] T. He, Z.R. Chong, J. Zheng, Y. Ju, and P. Linga. Lng cold energy utilization: Prospects and challenges. *Energy*, 170:557–568, March 2019. doi: 10.1016/j.energy.2018.12.170.
- [42] H.O. Njoku, O.V. Ekechukwu, and S.O. Onyegegbu. Analysis of stratified thermal storage systems: An overview. *Heat Mass Transfer*, 50, 2014. doi: 10.1007/s00231-014-1302-8.
- [43] I. Dincer and M.A. Ezan. *Heat Storage: A Unique Solution For Energy Systems*. Springer, Cham, 2018. doi: 10.1007/978-3-319-91893-8_3.
- [44] K.H. Chua, Y.S. Lim, and S. Morris. Energy storage system for peak shaving. *International Journal of Energy Sector Management*, 10(1):3–18, 2016. doi: 10.1108/IJESM-01-2015-0003.
- [45] Yongjun Sun, Shengwei Wang, Fu Xiao, and Diance Gao. Peak load shifting control using different cold thermal energy storage facilities in commercial buildings: A review. *Energy Conversion and Management*, 71:101–114, 2013. doi: 10.1016/j.enconman.2013.03.026.
- [46] Mohd Amin Abd Majid, Masdi Muhammad, Chima Cyril Hampo, and Ainul Bt Akmar. Analysis of a thermal energy storage tank in a large district cooling system: A case study. *Processes*, 8(9), September 2020. doi: 10.3390/pr8091158.
- [47] Binjian Nie, Anabel Palacios, Boyang Zou, Jiayu Liu, Tongtong Zhang, and Yunren Li. Review on phase change materials for cold thermal energy storage applications. *Renewable and Sustainable Energy Reviews*, 134:110340, 2020. doi: 10.1016/j.rser.2020.110340.

